CHANGES IN PERMEABILITY CAUSED BY TRANSIENT STRESSES: FIELD OBSERVATIONS, EXPERIMENTS, AND MECHANISMS

Michael Manga,[1] Igor Beresnev,[2] Emily E. Brodsky,[3] Jean E. Elkhoury,[4] Derek Elsworth,[5] S. E. Ingebritsen,[6] David C. Mays,[7] and Chi-Yuen Wang[1]

[1] Oscillations in stress, such as those created by earthquakes, can increase permeability and fluid mobility in geologic media. In natural systems, strain amplitudes as small as 10^{-6} can increase discharge in streams and springs, change the water level in wells, and enhance production from petroleum reservoirs. Enhanced permeability typically recovers to prestimulated values over a period of months to years. Mechanisms that can change permeability at such small stresses include unblocking pores, either by breaking up permeability-limiting colloidal deposits or by mobilizing droplets and bubbles trapped in pores by capillary forces. The recovery time over which permeability returns to the prestimulated value is governed by the time to reblock pores, or for geochemical processes to seal pores. Monitoring permeability in geothermal systems where there is abundant seismicity, and the response of flow to local and regional earthquakes, would help test some of the proposed mechanisms and identify controls on permeability and its evolution.

1. INTRODUCTION

[2] The permeability of Earth's crust is of great interest because it largely governs key geologic processes such as advective transport of heat and solutes and the generation of elevated fluid pressures by processes such as physical compaction, heating, and mineral dehydration. For an isotropic material, permeability k is defined by Darcy's law that relates the fluid discharge per unit area q to the gradient of hydraulic head h,

$$\mathbf{q} = -\frac{kg\rho}{\mu}\nabla h, \qquad (1)$$

where ρ is the fluid density, μ the fluid viscosity and g is gravity. The permeability of common geologic media varies by approximately 16 orders of magnitude, from values as low as 10^{-23} m^2 in intact crystalline rock, intact shales, and fault cores, to values as high as 10^{-7} m^2 in well-sorted gravels. Nevertheless, despite being highly heterogeneous, permeability can be characterized at the crustal scale in a manner that provides useful insight [e.g., *Gleeson et al.*, 2011].

[3] The responses of hydrologic systems to deformation provide some insight into controls on permeability, in particular its evolution in time. For example, the water level in wells and discharge in rivers have both been observed to change after earthquakes. Because earthquakes produce stresses that can change hydrogeologic properties of the crust, hydrologic responses to earthquakes are expected, especially in the near field (within a fault length of the

[1]Department of Earth and Planetary Science, University of California, Berkeley, California, USA.

[2]Department of Geological and Atmospheric Sciences, Iowa State University, Ames, Iowa, USA.

[3]Department of Earth and Planetary Sciences, University of California, Santa Cruz, California, USA.

[4]Department of Civil and Environmental Engineering, University of California, Irvine, California, USA.

[5]Department of Energy and Mineral Engineering, Center for Geomechanics, Geofluids, and Geohazards, EMS Energy Institute, Pennsylvania State University, University Park, Pennsylvania, USA.

[6]U.S. Geological Survey, Menlo Park, California, USA.

[7]Department of Civil Engineering, University of Colorado Denver, Denver, Colorado, USA.

Corresponding author: M. Manga, Department of Earth and Planetary Science, University of California, 307 McCone Hall, Berkeley, CA 94720, USA. (manga@seismo.berkeley.edu)
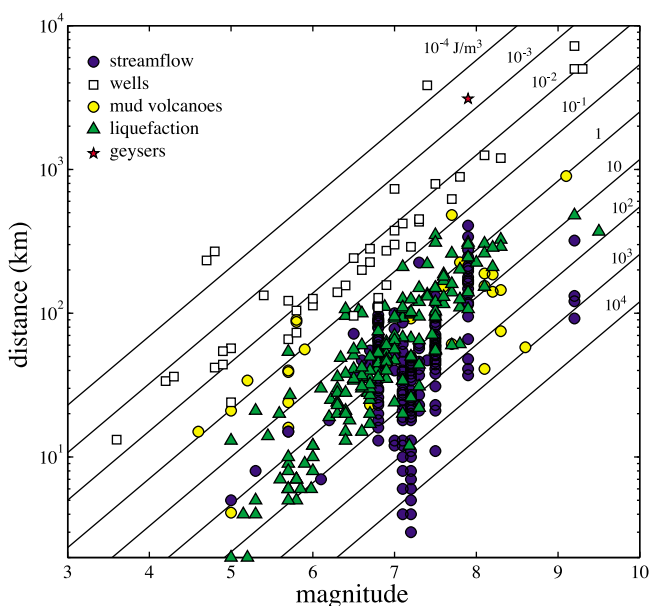
Figure 1. Distribution of earthquake-induced hydrologic changes as functions of earthquake magnitude and epicentral distance. Also plotted are the contours of constant seismic energy density e, given by equation (1), which is the seismic energy per unit volume responding to the seismic wave train; it thus represents the maximum seismic energy available to do work at a given location. Data compiled and tabulated in *Wang and Manga* [2010b].

ruptured fault) where transient (temporary) and static (permanent) stress changes are both large. What is unexpected is the great distance over which these phenomena occur—up to thousands of kilometers away from the earthquake epicenter, distances we refer to as intermediate field (one to a few fault lengths away from the fault) to far field (many fault lengths). At such large distances the static stress changes caused by slip on the ruptured fault are far too small to explain these observations (these stresses are much smaller than stresses from tides or weather, for example). Instead, dynamic stresses, i.e., shaking, must be invoked. As there is no permanent deformation caused by the passage of seismic waves, transient stresses must be translated into changes in subsurface structure and hydrogeologic properties that persist far longer than the duration of shaking. While the observed hydrological responses are sometimes viewed as little more than curiosities, they indicate that small transient stresses can result in transient or persistent changes in hydrogeologic properties and hydrological processes.

[4] Many of the hydrological responses to earthquakes are most easily explained by changes in permeability or fluid mobility, that is, k or the group of terms in front of ∇h in equation (1), respectively. This suggests that stimulation with low-amplitude stresses could be used in engineered systems to enhance fluid flow. Indeed, the use of stimulation through the application of vibrations has a long history of study for enhanced oil recovery [e.g., *Beresnev and Johnson*, 1994; *Nikolaevskiy et al.*, 1996; *Kouznetsov et al.*, 1998; *Roberts et al.*, 2003]. Despite widespread documentation of hydrologic responses in the field, however,

the mechanism or mechanisms by which permeability changes are uncertain. This limits the ability to evaluate whether stimulation would be effective in engineered systems where permeability is critically important, for example, to maintain permeability in enhanced geothermal systems (EGS).

[5] There are several open questions relevant for both understanding the natural phenomena and for engineering applications:

[6] 1. What are possible pore- and fracture-scale mechanisms for permeability changes? Are new pathways being created? Or, are existing paths being unclogged?

[7] 2. Is there a frequency dependence, and if so, what does this reveal about processes that change permeability?

[8] 3. Does permeability always increase?

[9] 4. Dynamically increased permeability seems to return to its prestimulated value. What controls the recovery time of permeability?

[10] 5. What materials are the most sensitive? Is there a threshold for hydraulic response in terms of strain amplitude or hydrodynamic shear?

[11] 6. Can dynamic stresses be used to maintain permeability in EGS? Can monitoring of productive geothermal reservoirs provide insights into permeability evolution? Questions 2–5 all address the mechanisms by which permeability changes.

[12] We focus in this review on observations that indicate that relatively small (<1 MPa) transient stresses change fluid flow and fluid pressure, and on mechanisms that can explain these observations. We do not address changes in permeability that arise from the application of stresses large enough to cause shear failure or create hydrofractures in intact rock, typically at least several MPa. We do, however, compare the magnitude of permeability changes caused by transient stresses with those produced by shear and tensile failure of rock.

[13] We begin in section 2 by reviewing the response of natural hydrological systems to earthquakes and the evidence that for some of these responses, permeability changed in response to the transient stresses rather than the coseismic static stresses. In section 3, we discuss insights obtained from experiments in which permeability was measured under water-saturated conditions before and after the application of transient stresses. Both the laboratory and field observations indicate that stresses too small to produce new cracks or pathways are able to change permeability. Instead, preexisting pathways that are clogged may be cleared by the transient flows produced by transient stresses. Recent studies also show that the earthquake-enhanced permeability (increased k) may recover with time to the preseismic value. We thus tabulate the documented time for the permeability recovery, which may bear on the mechanism of the recovery processes. In section 4 we consider two classes of processes that can explain how small changes in stress could change permeability: (1) mobilization of colloidal deposits and (2) mobilization of pore-blocking nonwetting bubbles or droplets. We also discuss mechanical and geochemical processes as mechanisms for the permeability recovery. In section 5 we place the permeability changes
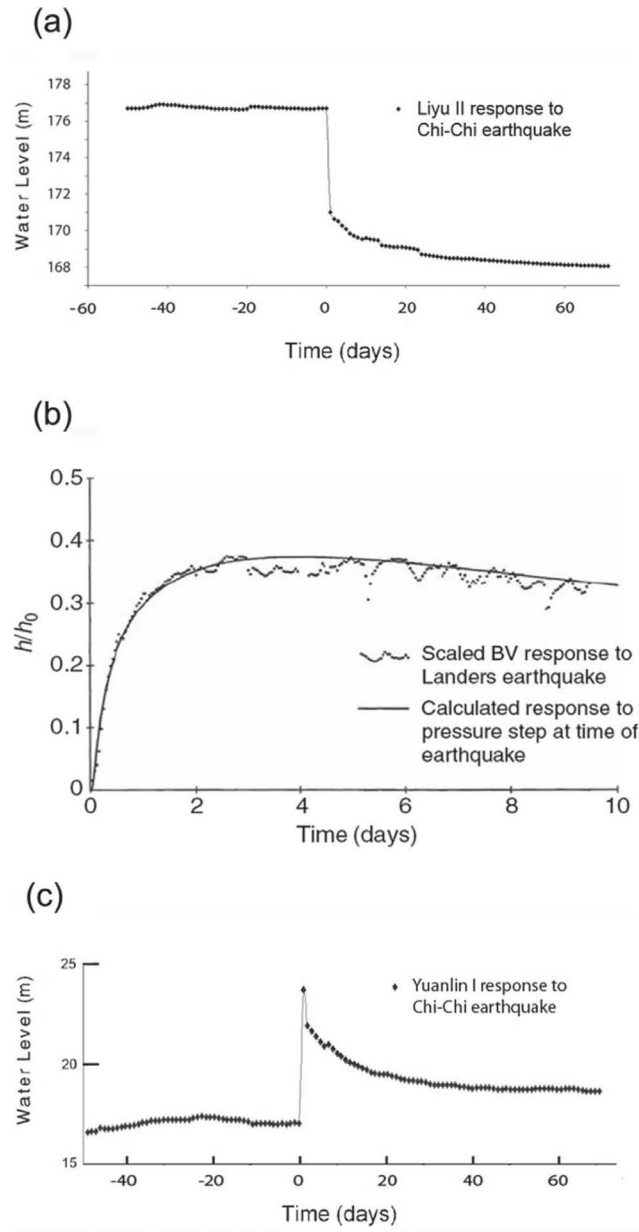
Figure 2. (a) Water level decrease in the Liyu II well during the 1999 M_w7.5 Chi-Chi earthquake (occurring at t = 0) in Taiwan. The well is ~5 km from the surface rupture of the causative fault. The step-like coseismic water level decrease is −5.94 m. (b) Scaled groundwater level response of well BV in central California to the 1992 M 7.3 Landers earthquake 433 km from the well. The observed water level changes, shown with data points, can be modeled by a coseismic, localized pore pressure change at some distance from the well, shown by the solid curve. (c) Water level increase in Yuanlin well during the 1999 M_w7.5 Chi-Chi earthquake (occurring at time = 0). The well is ~25 km from the hypocenter, thus in the near field, and ~13 km from the surface rupture of the causative fault. The step-like coseismic water level increase is +6.55 m. Figures 2a and 2c are from *Wang and Chia* [2008], and Figure 2b is from *Roeloffs* [1998].

generated by earthquakes in geological context. First, we compare the magnitude of permeability changes generated by small transient stresses with those generated by tectonic activity or EGS. Second we discuss the possible relevance of stress-induced changes in permeability for the triggering of earthquakes by other earthquakes. We end this review by revisiting the questions listed in this introduction.

2. RESPONSE OF NATURAL SYSTEMS TO EARTHQUAKES

[14] It has long been documented that earthquakes induce hydrologic responses in surface water and groundwater (e.g., Pliny the Elder's *Historia Naturia*, Book 31, chapter 30). Examples include changes in stream flow, changes in the level, temperature and geochemistry of water in wells, changes in the productivity of oil wells, and liquefaction.

[15] The compilation in Figure 1 shows that there is a clear relationship between earthquake magnitude and the distance over which hydrological responses have been documented. A subset of these responses has been attributed to changes in permeability. In the following subsections we briefly discuss the nature of some of these responses and the evidence that some may be the result of increased permeability.

2.1. Wells

[16] Water wells show multiple types of responses to earthquakes. Water level changes are commonly recorded and might indirectly indicate permeability enhancement. Other relatively rare observations, like tidal or seismic wave responses, more directly measure permeability changes.

[17] Water level changes in wells are the most widely reported hydrologic response to earthquakes. Using records from a single well in central California that responded to multiple earthquakes, *Roeloffs* [1998] identified distinct types of groundwater level responses. In the near field (within one fault length of the fault), groundwater level showed step-like increases (Figure 2c). In the intermediate field (distances of one to a few fault lengths), groundwater level changes were more gradual and persisted for hours to weeks (Figure 2b). At even greater distances (the far field), only transient oscillations of groundwater level were documented. The transient oscillations can occur at distances of thousands of kilometers from the epicenter and arise from a resonance between water flowing into and out of the well with water level oscillations within the well [*Cooper et al.*, 1965; *Liu et al.*, 1989].

[18] *Jónsson et al.* [2003] documented a pattern of coseismic changes in water level in the near field following a 2000 M 6.5 strike-slip earthquake in Iceland that agreed with the pattern of calculated pore pressure changes created by coseismic volumetric strain. However, coseismic static strain is not the only control on changes in water level, even in the near field. The dense network of hydrological wells in central Taiwan allowed a critical test of the common hypothesis that the coseismic change in water level is a result of volumetric strain. Following the 1999 M 7.5 Chi-Chi earthquake, the water level rose in most wells where the coseismic volumetric strain is dilatation, and fell in other wells where the
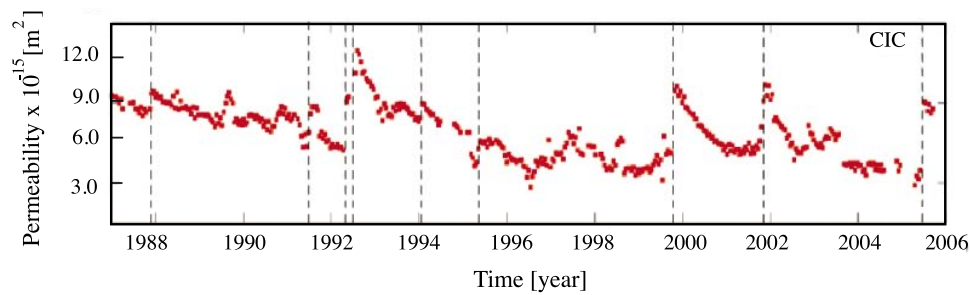
Figure 3. Change in permeability based on water level responses to semidiurnal tides for the water levels at a well in southern California. Transient changes of inferred permeability are clearly evident at the time of earthquakes, shown by the vertical lines (permeability is calculated from the phase data shown in *Elkhoury et al.* [2006]). The magnitude of permeability change is linearly proportional to the peak ground velocity.

volumetric strain is contraction [*Koizumi et al.*, 2004]. This is in direct contradiction to the pattern predicted from coseismic volumetric strain; that is, contraction should have led to groundwater level increases and dilatation to groundwater level decreases. *Wang et al.* [2001] proposed instead that coseismic increases in water level in the near field are caused by sediment consolidation under seismic shaking and the decreases in water level were due to sediment dilatation related to fracture formation near the ruptured fault (Figure 2a). Thus the mechanisms responsible for the observed groundwater level changes in these confined aquifers may depend critically upon local geologic conditions: unconsolidated sediments in Taiwan versus fractured basalt in Iceland.

[19] The processes leading to water level changes in the intermediate to far field are uncertain. At these distances, static stress changes are small and hydrological responses are most likely initiated by transient stresses from the seismic waves. *Roeloffs* [1998] suggested that gradual changes in water level are caused by a coseismic, localized pore pressure change at some distance from the well. *Brodsky et al.* [2003] proposed that Rayleigh wave–induced groundwater flow enhanced permeability that in turn led to a redistribution of pore pressure. *Wang et al.* [2009] found that S waves and Love waves may also change water level, even though there are no apparent transient volumetric strains associated with these waves, and appealed to permeability changes driven by groundwater flow induced by the transient stresses. Documenting the relationship between water level changes and permeability in natural systems requires incorporating evidence from more direct indicators of permeability changes in natural systems.

[20] Occasional high-frequency measurements of water level have revealed a different set of tools to probe natural permeability and its evolution. Both seismic waves and tidal strains can impose known, well-calibrated quasi-static dilatational strains on aquifer-well systems. As the same strain is applied to the aquifer and the well, different pore pressure responses occur in the aquifer than in the open well owing to the difference in storage. The resultant pressure gradient drives a flow in and out of the well. The amplitude of the driven water level oscillations increases with increasing

permeability as the water can more easily flow to the well. *Brodsky et al.* [2003] recorded such an increase in water level oscillations driven by seismic waves, which they interpreted as a relatively direct indication of a permeability increase. Since a water level drop accompanied this permeability increase, a link was made between permeability enhancement and water level changes.

[21] In a complementary study, *Elkhoury et al.* [2006] documented decreases in the phase of the response to semidiurnal tides coincident with many regional earthquakes. These changes are most easily explained by an earthquake-enhanced permeability. The phase lag between the imposed tidal strain and the resulting water level oscillations decreases as permeability increases. The change in phase lag can be translated into permeability by using a specific hydrological model, and one example well is shown in Figure 3. *Elkhoury et al.* [2006] found that the change in permeability scaled linearly with the peak ground velocity, at least in the range of recorded values, showing that the magnitude of transient stresses is related to the magnitude of hydrogeological response.

2.2. Stream and Spring Discharge

[22] For practical reasons, discharge in streams and at springs has been monitored for a long time, and the typical earthquake response of streams not affected by impoundment by landslides is an increase of discharge [*Muir-Wood and King*, 1993]. Available stream gauge records show that the onset of the streamflow increase is coseismic, but it can take days or even weeks for the increase to reach its maximum (Figure 4).

[23] For example, after the 1989 Loma Prieta earthquake in central California, a network of U.S. Geological Survey stream gauges documented widespread increases of stream discharge in the near and intermediate field. In addition, *Rojstaczer and Wolf* [1992] reported marked increases in the concentration of the major ions in the stream water after the earthquake, with the proportions of major ions nearly the same as those before the earthquake. They also observed that temperature of the stream water after the earthquake was several degrees lower than under normal conditions. These observations led the authors to conclude that the increased
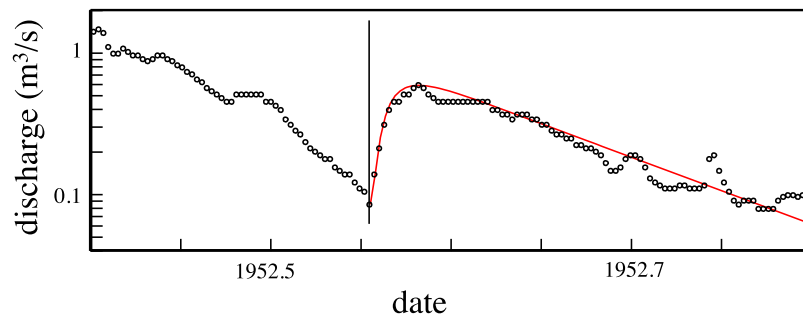
Figure 4. Response of Sespe Creek in California to the 1952 *M* 7.5 Kern County earthquake. Daily average discharge measurements collected and archived by the U.S. Geological Survey are shown with circles. Vertical line shows the time of the earthquake. No precipitation occurred during the time interval shown. Curve is the solution to a model in which vertical permeability increases at the time of the earthquake [*Wang et al.*, 2004]. Figure adapted from *Manga et al.* [2003].

discharge was caused by earthquake-enhanced permeability. Increased permeability was invoked for other cases where stream and spring discharge increased [e.g., *Briggs*, 1991; *Tokunaga*, 1999; *Sato et al.*, 2000].

[24] Using discharge records from a single stream in southern California that responded to multiple earthquakes, *Manga et al.* [2003] showed that streamflow at this site always increased after an earthquake whether or not the static, local crustal stress induced by the earthquake caused contraction or dilatation. The lack of correlation of responses with static stress and a correlation with dynamic stresses led *Manga et al.* [2003] to conclude that it must be the transient stresses, rather than static stresses, that caused the responses. Other studies draw similar conclusions based on the lack of correlation between the sign of the static volumetric stresses and the sign of the discharge response [*Manga and Rowland*, 2009; *Cox et al.*, 2012]. Further, analysis of the recession characteristics of streams showed no seismically induced changes in base flow recession [e.g., *Manga*, 2001; *Montgomery et al.*, 2003] implying little change in horizontal basin-scale permeability. Instead, *Wang et al.* [2004], based on an analysis of streamflow responses to the 1999 Chi-Chi earthquake, suggested that the increased streamflow was due to an earthquake-enhanced *vertical* permeability in the nearby mountains, which led to increased recharge of the aquifers that feed the streams. Abundant subvertical fractures were mapped after the earthquake in areas near the surface rupture [*Lee et al.*, 2002], and may have caused the increased vertical permeability. The horizontal permeability of aquifers, which is typically higher, was not significantly affected by these fractures. Because stream discharge integrates the response of the local watershed, it is not possible from a single gauge or spring to determine whether changes in permeability are localized or widespread.

[25] Because there are few documented examples of streams and springs that have responded multiple times to earthquakes, it is difficult to identify whether the magnitude of the transient stresses scales with the magnitude of discharge changes. The stream studied by *Manga et al.* [2003] showed a response that scaled with the magnitude of

transient stresses. However, the springs studied by *King et al.* [1994] and *Manga and Rowland* [2009] had a response of similar magnitude following all earthquakes. More data is clearly needed.

2.3. Liquefaction

[26] Along the spectrum of natural hydrologic response to earthquakes, liquefaction is the most easily recognized in the field and, for this reason, one of the earliest to be thoroughly documented [*Seed*, 1968; *China Earthquake Administration*, 1976; *National Research Council*, 1985; *Ambraseys*, 1988; *Galli*, 2000]. Liquefaction can occur when solids are rearranged into a more compact arrangement, so that the reduction in pore volume increases fluid pressure in the pore space. Liquefaction following earthquakes is associated with high pore pressure in the subsurface, as evidenced by the common association of liquefaction with the expulsion of mixtures of liquefied sand and water to substantial heights above the surface. The most commonly liquefied sediments are fine sands and silts, although liquefied gravely sediments have increasingly been reported [*Youd et al.*, 1985; *Kokusho*, 2007].

[27] It has also been recognized that liquefaction requires confined conditions to allow pore pressure to build up during seismic shaking. A field experiment conducted at the Wildlife Liquefaction Array in southern California [*Holzer et al.*, 1989], with measurements of both pore pressure and intensity of ground motion, demonstrated that earthquake-induced liquefaction in the field is a progressive process that includes a gradual buildup of pore pressure and a progressive softening of sediments with increasing cycles of seismic loading, until the rigidity is reduced to zero [*Holzer and Youd*, 2007]. Using strong motion records in central Taiwan during the 1999 Chi-Chi earthquake, *Wang et al.* [2003] and *Wong and Wang* [2007] showed that the occurrence of liquefaction correlates more strongly with low-frequency seismic waves (≤1 Hz) than with high-frequency seismic waves.

[28] Many studies have proposed empirical relationships for the maximum epicentral distance of liquefaction sites, i.e., the threshold distance, as a function of earthquake

magnitude [*Kuribayashi and Tatsuoka*, 1975; *Ambraseys*, 1988; *Papadopoulos and Lefkopoulos*, 1993; *Galli*, 2000]. Combining this empirical relationship with an empirical relationship between seismic energy and earthquake magnitude, *Wang* [2007] suggested that these two parameters (distance to earthquake D and earthquake magnitude M) may be replaced by a single physical parameter, the seismic energy density e

$$\log_{10}e = -3\log_{10}D + 1.5M - 4.2, \qquad (2)$$

with D in kilometers and e in J/m^3. Thus contours of constant e plot as straight lines on a log D versus M diagram (Figure 1). The threshold seismic energy density required for liquefaction coincides with the contour $e \sim 0.1$ J/m^3. This is at least 2 orders of magnitude lower than the energy density required to liquefy the most sensitive sediments by undrained consolidation in the laboratory, $\sim$30 J/m^3 for well-sorted clean sands [*Green and Mitchell*, 2004]. Since the latter energy density is comparable to the threshold seismic energy density in the near field [*Wang*, 2007], the prevailing model (liquefaction caused by undrained consolidation) may be valid in the near field and may explain the majority of observations plotted in Figure 1. Liquefaction at greater distances, however, would require a different mechanism. *Wang* [2007] proposed that enhanced permeability allows hydraulically isolated regions with high pore pressure but low liquefaction potential to connect with the units that liquefy. *Cox et al.* [2012] similarly suggest that enhanced groundwater flow may have contributed to the extensive liquefaction in New Zealand after the 2010 Darfield earthquake. If this is correct, then changes in permeability may play a role in liquefaction in field settings. This hypothesis needs further field and laboratory study. It implies that characterizing deeper subsurface aquifers may be relevant for assessing liquefaction potential.

2.4. Change in Temperature and Composition of Groundwater

[29] Given that earthquakes can change groundwater flow, changes in the temperature and composition of groundwater are expected. On this topic there are far fewer quantitative data and these often have very limited temporal resolution. *Mogi et al.* [1989] documented increases in temperature of $\sim$1°C in an artesian thermal well in the northeastern part of the Izu Peninsula, Japan following far-field earthquakes. The temperature changes vary from earthquake to earthquake and the magnitude of the changes are not clearly correlated with the amplitude of stresses. *Mogi et al.* [1989] suggested that seismic waves dislodged precipitates in the pore space, increasing the flux of geothermal water and causing temperature to suddenly rise.

[30] After the 1999 Chi-Chi earthquake in Taiwan, temperature changes were documented in wells located on an alluvial fan. A group of wells located on the upper rim of the alluvial fan in the near field showed widespread decreases in temperature of $\sim$1°C after the earthquake, suggesting increased recharge owing to enhanced permeability [*Wang et al.*, 2012].

[31] The temperature of geothermal vents at mid-oceanic ridges shows both positive [*Johnson et al.*, 2000] and negative [*Dziak et al.*, 2003] coseismic changes. These have been interpreted to result from the opening of clogged fractures that enhances permeability and flow between reservoirs at different temperatures. *Davis et al.* [2001] recorded transient changes of both temperature and pore pressure in boreholes on the eastern flank of the Juan de Fuca Ridge in response to an earthquake swarm. While pore pressure changed only during the first earthquake of the swarm, temperature also changed after many of the later earthquakes. *Wang and Manga* [2010b] interpreted this observation as reflecting a difference in the required recovery time. Pore pressure response to the first earthquake may be due to opening of clogged cracks and redistribution of pore pressure, and permeability may not have enough time to recover (and pore pressure to rebuild) before the later earthquakes. On the other hand, the transient temperature changes may be caused by seismically triggered turbulent mixing of water column in the well [*Shi et al.*, 2007], which readily comes into thermal equilibrium with the wall rock between earthquakes.

[32] Study of changes in groundwater composition is also hampered by the scarcity of quantitative data. Nevertheless, coseismic changes in dissolved ions [e.g., *Tsunogai and Wakita*, 1995; *Biagi et al.*, 2006] and radon flux [e.g., *Wakita et al.*, 1989] have been reliably documented. The most comprehensive study to date is probably that by *Claesson et al.* [2004, 2007], who documented the change in groundwater composition in northern Iceland after a large earthquake in 2002. The authors showed that the concentrations of 12 ionic species and the stable isotopes of oxygen (δ^{18}O) and hydrogen (δD) all changed after the earthquake. Plotting δ^{18}O against δD for the groundwater samples, the authors found the direction of the changes to be parallel to the Global Meteoric Water Line, implying that the changes were due to mixing of pore waters among shallow aquifers. They attributed this to earthquake-enhanced permeability.

[33] Although most documented temperature changes occurred in the near field, some changes in temperature [*Mogi et al.*, 1989] did occur in the far field [*Wang and Manga*, 2010b]. Another common response of wells and springs to far-field earthquakes is an increase in turbidity [e.g., *Waller et al.*, 1965; *Whitehead et al.*, 1984; *King et al.*, 1994] that can persist for weeks [e.g., *Coble*, 1965]. *Borg et al.* [1976] also documented temporary increases in turbidity in wells and water level, 50–115 km from the sites of nuclear weapon tests. The increased turbidity apparently resulted from clay-sized particles being flushed from aquifers —it is possible that mobilization of these particles increases permeability by unclogging pore space.

2.5. Recovery Time Scales

[34] The recovery of earthquake-enhanced permeability to the preseismic value, as documented by recent studies and compiled in Table 1, may have important implications for postseismic groundwater flow and the related transport of

TABLE 1. Postseismic Recovery of Crustal Permeability

Type of Observation	Locality	Depth	Time to Recovery	Time of Observation	References
Groundwater level response to earthquake	South Taiwan	200 m	3 min[a]	2008	Geballe et al. [2011]
Groundwater level response to tides	Pinon Flat, S. California	0–200 m	Days to months	1988–2006	Elkhoury et al. [2006]
Springs, temperature chemistry	Alum Rock, California	Surface	months to >1.5 years[a]	2003–present	Manga and Rowland [2009]
Pore pressure repose time	Juan de Fuca Ridge, Pacific Ocean	Ocean bottom	>100 days	1999	Davis et al. [2001], Wang and Manga [2010b, chapter 6]
Streamflow response to earthquakes	Coastal Range of southcentral Chile	Surface	>300 days	2010–2011	Mohr et al. (submitted manuscript, 2011)
Groundwater chemistry	Iceland	1.2 km	~2 years	1995–2004	Claesson et al. [2004, 2007]
Mud volcano repose time	Azerbaijan Niikappu, Japan	undetermined	~2 years	1848–1902 1952–1973	Mellors et al. [2007], Manga et al. [2009]
Water injection, numerical modeling	Matsuhiro, Japan	2 km	3–5 years	1965–1970	Ohtake [1974], Cappa et al. [2009]
Repeated water injection	Nojima, Japan	1.8 km	6 years	1997–2003	Kitagawa et al. [2007]

[a]Indicates that time scales are based on time for anomaly to decay by a factor of e; otherwise recovery times are based on observed time to return to conditions similar to those prior to the earthquake.

heat and solutes [e.g., *Wang et al.*, 2012]. Recovery may also provide insights into the mechanism of the permeability enhancement. Permeability recovery has been documented in a wide range of settings, from deep ocean basins [*Davis et al.*, 2001] to small drainage basins near the crest of Coast Range of the Andes Mountains (C. Mohr et al., Streamflow response in small upland catchments in the Chilean Coastal Range to the 8.8 M_w Maule Earthquake on February 27, 2010, submitted to *Journal of Geophysical Research*, 2011). The mechanism for this recovery is unclear, but may be due to some combination of mechanical, biochemical and geochemical processes that reblock the fluid pathways cleared by the seismic shaking during the last earthquake. As Table 1 shows, most documented recovery times are about 2 years, but range from as short as 3 min, the exponential decay time in *Geballe et al.* [2011], to 6 years [*Kitagawa et al.*, 2007]. *Ingebritsen and Manning* [2010] inferred from modeling crustal-scale permeability that enhanced permeability in dynamic geologic environments may decay over a time scale of 10^0–10^3 years. We note a possible observational bias in this compilation of values: shorter times may not be captured, and recognizing longer times requires long monitoring periods. Any relationship between permeability recovery and aquifer recharge has not been established. Furthermore, the apparent duration of the recovery may be influenced by the magnitude of the original enhancement, but the data are not sufficient to assess this possibility.

3. LAB EXPERIMENTS

[35] Laboratory experiments provide an opportunity to document responses to transient stresses with controlled amplitude and frequency. While the scale is much smaller than that for field settings (section 2) in which hydrogeological properties are expected to be spatially variable, the scale is still much larger than the pore scale at which permeability-controlling processes may operate. The laboratory experiments are thus not a direct probe of pore-scale mechanisms. Here we review laboratory experiments that applied transient stresses to induce changes in permeability for the case of single-phase fluid flow. Experiments show both increases and decreases in permeability. Features of the experiments are summarized in Table 2.

[36] *Elkhoury et al.* [2011] investigated the influence of pore pressure oscillations on the effective permeability of rocks fractured after placement in an experimental apparatus. Samples of intact Berea sandstone were fractured in a triaxial deformation apparatus. Flow of deionized water was established via independently servo-controlled pore pressures at the inlet and outlet. After the fluid flow had reached steady state, 6 sinusoidal pore pressure oscillations with 20 s periods were applied at the inlet while keeping the outlet pressure constant. The total effective permeability, k, was used as an interpretive tool to monitor the response of the fractured sample. Immediately after the oscillation, k increased and then decayed to the prestimulation value over a time scale of tens of minutes. Measurements at the inlet

TABLE 2. Descriptions of Experimental Conditions and Results of the Four Experiments Presented in Section 3

Experiments	Frequency (Hz)	Peak Amplitude	Oscillations	Samples	Permeability Response	Recovery	Response Type
Elkhoury et al. [2011]	0.05	0.02–0.3 MPa	Pore Pressure	Fractured in situ	Increase	10 s min	Transient
Liu and Manga [2009]	0.3–2.5	Strain 10^{-4}	Axial Displacement	Fractured	Decrease	No recovery	Permanent
Roberts [2005]	25–75	0.3–1.2 MPa	Axial Stress	Intact	Increase	Immediate	Transient
Shmonov et al. [1999]	0.05–20	Strains 10^{-4}–10^{-3}	Axial stress	Intact	Decrease (low T) increase (high T)	Not documented	Not documented

and outlet showed the same effect, which is important because it demonstrates a permeability change rather than a transient storage effect associated with the poroelastic response of the system. That is, it is the ability to transmit, rather than store, fluids that change. Figure 5 shows that pore pressure oscillations can have a large effect on permeability, with the increase in permeability increasing exponentially with the amplitude of the pressure oscillations. Interestingly, the collapse of normalized permeability changes shown in Figure 5 to a single curve implies that less permeable rocks are no more sensitive to transient stresses than more permeable rocks. Additional experiments were performed on samples fractured outside the apparatus and then assembled for the flow through. In these instances no changes in permeability were observed after stimulation.

[37] *Shmonov et al.* [1999] applied oscillatory stresses to unfractured cores at high confining pressures and temperatures. Strain amplitudes were between 10^{-4} and 10^{-3}, frequencies from 0.05 to 20 Hz, and the duration of the stressing was >15 min. At low temperatures they typically found small permeability decreases of a few percent, and in one case a threefold decrease after 40 min of stressing. At high temperatures, they found that permeability was more likely to increase, by as much as a factor of 3.7. *Liu and Manga* [2009] performed similar experiments on already-fractured sandstone cores saturated with deionized water, but using only 5–10 cycles of deformation. Permeability was first measured with steady flow. Transient stresses were imposed by oscillating the axial displacement to achieve strain amplitudes of 10^{-4} with frequencies from 0.3 to 2.5 Hz. Additional experiments were performed with natural silt particles injected into the fractures, motivated by suggestions that permeability changes are the result of mobilized particles [e.g., *Mogi et al.*, 1989; *Brodsky et al.*, 2003; *Elkhoury et al.*, 2006]. In general, permeability decreased after each set of oscillations and the decreases were progressively smaller with each additional application of transient stress. Furthermore, samples with the added silt showed the largest decrease in permeability in response to the oscillatory stresses. The magnitudes of permeability changes were similar to those found by *Shmonov et al.* [1999] where the duration of the applied dynamic stressing was more than 260 times greater than in *Liu and Manga* [2009]. This suggests that a few cycles of dynamic stimulation are sufficient to induce the observed changes in permeability. No recovery of permeability was documented within ~10 min of the stimulation.

[38] *Roberts* [2005] studied the influence of axial stress oscillations in single-phase and two-phase flow experiments on intact sandstone cores. Transient stress was imposed with sinusoidal cycling of axial stresses. The single-phase flow experiment started with one pore volume of fresh water (low ionic strength) and resulted in a 20% decrease of permeability. This was attributed to the release of clay particles that clogged pore throats. After steady state had been reached, continuous dynamic stressing was applied with frequency of 50 Hz and amplitude of 0.3 MPa. There were no observable effects on permeability. Then the amplitude of the continuous stress cycling was increased to 0.6 MPa after which permeability increased 15%. A further increase in the amplitude of stress cycling to 0.9 MPa added another 5% increase in permeability. Upon stopping the dynamic stimulation, permeability returned to prestimulation values.

[39] These experiments all show that transient stresses can change permeability, provided the stress amplitudes are large enough. The observed differences in these experiments are presumably due to some combination of (1) the fracturing procedure, (2) the type of applied stresses (oscillation of
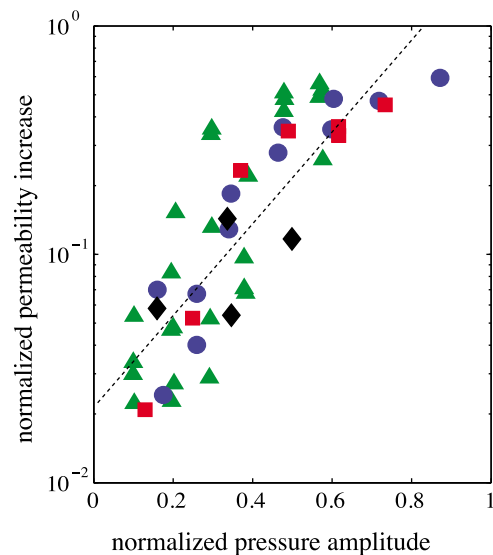
Figure 5. Permeability increase measured in the laboratory as a function of imposed pore pressure oscillation amplitude. Permeability changes are normalized by permeability before the oscillations; pressure amplitudes are normalized by the pore pressure difference driving the flow. Different symbols and colors correspond to different samples. Modified from *Elkhoury et al.* [2011].

pore pressure or axial strains or axial stresses), and (3) differences in the frequency of the oscillations that span 0.05–75 Hz. It is important to note that in all these experiments, the magnitude of the transient strains is at the high end of those that cause permeability to change in natural systems. Natural systems respond to strain amplitudes as small as $\sim10^{-6}$; in the experiments, strain amplitudes are 10^{-4}–10^{-3} [*Shmonov et al.*, 1999], 10^{-4} [*Liu and Manga*, 2009], 10^{-4} [*Roberts*, 2005], and 10^{-5}–10^{-4} [*Elkhoury et al.*, 2011]. The equivalent stresses are up to about one MPa, but low enough that shear and tensile failure do not occur; for example, *Liu and Manga* [2009] and *Elkhoury et al.* [2011] found that their sandstone cores failed for axial stresses of 30 MPa, about 2 orders of magnitude greater than the transient stress amplitudes in their experiments. Where rocks are already confined by compressive in situ stresses, the applied stress excursions will be even further from inducing failure.

4. MECHANISMS

[40] We now address possible mechanisms for the permeability changes and recovery documented in the field and laboratory. Specifically, how can small oscillations in stress change permeability? We address only mechanisms that do not require creating new fractures.

4.1. Mechanisms That Enhance Permeability

4.1.1. Particle Mobilization

[41] Several observations, for example, the changes in turbidity of groundwater (section 2.4), suggest that the transient stresses created by earthquakes change permeability by mobilizing colloids. Colloids, particles with equivalent diameters between 1 nm and 10 μm, include clay minerals, weathering and precipitation products, and environmental nanoparticles [*Hochella et al.*, 2012]. Colloids also include bacteria that can form biofilms that clog pore space, but here we confine ourselves to abiotic colloids controlled by mechanical and geochemical processes. Filtration of colloidal suspensions through porous media results in colloid deposition that can reduce permeability by up to 3 orders of magnitude [*Veerapaneni and Wiesner*, 1997; *Mays and Hunt*, 2007]. Conversely, mobilizing colloidal deposits can increase permeability.

[42] Deposition, mobilization, and permeability are coupled, but no predictive model is currently available that accounts for the broad diversity of natural porous media, colloids, and external stimulation. However, the roles of certain physical and chemical processes are widely recognized. Physical processes include erosion or restructuring of colloidal deposits by hydrodynamic forces and colloid sorption to an air-water interface [*Wan and Wilson*, 1994]. Chemical processes include decreases in ionic strength and increases in the concentration of oxidants that precipitate Fe and Mn solids. Determining which, if any, of these processes are active in natural systems is a challenge for understanding the role of transient stresses.

[43] Mechanical mobilization by flow driven by seismic waves is a plausible mechanism for colloidally mediated permeability changes. In analogous filtration problems, changes in fluid velocity mobilize previously deposited particles. For instance, *Cleasby et al.* [1963] reported that increases in rate of flow affect the mass of solids remobilized from a sand filter but found no effect of flow duration. *Ives and Pienvichitr* [1965] noted that intermittent sampling and variation in flow rate disturbed deposited materials. *Glasgow and Wheatley* [1998] investigated the effect of surging by comparing two sand filters with equal average flow rates, observing that the surging filter clogged more slowly and produced higher effluent turbidity. Increases in flow rate have been shown to remobilize previously deposited Giardia cysts [*Logsdon et al.*, 1981], PVC particles [*Bai and Tien*, 1997], polystyrene particles [*Bergendahl and Grasso*, 2000] and illite and kaolinite clay [*Gao et al.*, 2004]. Several other studies reported inadvertent particle mobilization: *Logsdon et al.* [1990] reported release of Cryptosporidium oocysts from a sand filter during filter startup; *Kessler* [1993] reported massive mobilization of Na-montmorillonite deposited in a model fracture after a power failure disturbed the flow rate; and *Backhus et al.* [1993] and *Gibs et al.* [2000] reported turbidity increases during groundwater sampling. The sensitivity of particle mobilization to changes in flow rate is not surprising, as some degree of particle mobilization is observed even without changes in the fluid velocity [*Kim and Tobiason*, 2004].

[44] Several studies have explored the relationship between periodic seismic stimulation and colloid mobilization, sometimes with corresponding measurements of permeability. Much of this work has focused on using ultrasonic stimulation to reduce particle clogging near well bores [e.g., *Poesio et al.*, 2004], but ultrasonic stimulation has limited relevance to earthquakes because such high-frequency waves are rapidly attenuated in natural porous media. Experiments with lower-frequency stimulation, from 26 to 150 Hz, have shown (1) enhanced transport of polystyrene microspheres through glass beads [*Thomas and Chrysikopoulos*, 2007], (2) mobilization of fines from Fontainebleau sandstone [*Roberts and Abdel-Fattah*, 2009], and (3) mobilization of polystyrene microspheres previously deposited on glass beads [*Beckham et al.*, 2010]. Permeability changes were not observed during mobilization of fines from sandstone, but were indicated by transient pressure drops during mobilization of microspheres from glass beads.

[45] In order to evaluate the plausibility of colloid mobilization as a mechanism for seismically driven permeability changes, we compare observations of mobilization with the hydrodynamic viscous shear stress, τ, applied to the colloid deposits,

$$\tau = \mu U/\delta, \qquad (3)$$

where μ is dynamic viscosity, U is the pore velocity, and δ is a characteristic pore size, calculated as $\delta = \sqrt{k/n}$ where k is permeability calculated from Darcy's law and n is porosity. In any particular situation, the critical hydrodynamic stress would presumably depend on the structure of the porous material, the colloids, the deposit structure, and the hydrodynamic forcing. A few studies have reported deposit shear
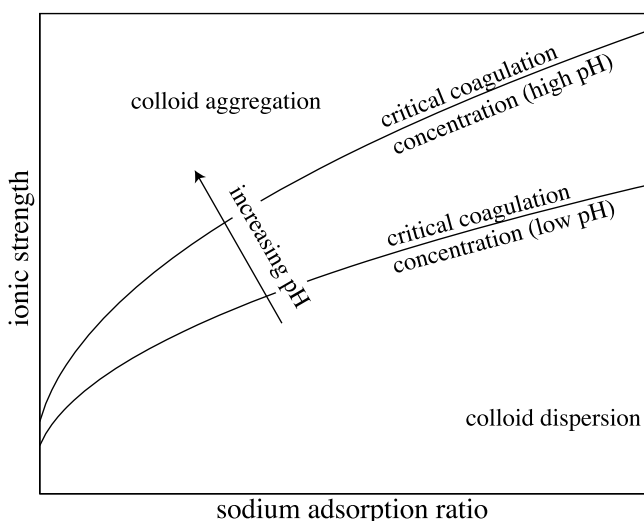
Figure 6. For a given type of colloid, the Quirk-Schofield diagram plots the critical coagulation concentration (CCC) as a function of ionic strength and sodium adsorption ratio (SAR) for a fixed value of pH. This diagram therefore provides a conceptual and quantitative model to distinguish chemical conditions favoring colloid dispersion, below the line for the relevant pH, versus colloid aggregation, above the line. Adapted from *Mays* [2007].

strength, above which colloid mobilization is observed in the specific configuration studied: $\tau = 0.27–0.4$ Pa for kaolinite in porous media [*Ives and Fitzpatrick*, 1989], and $\tau = 0.1–0.8$ Pa for Na-montmorillonite in fractures [*Kessler*, 1993]. *Mays and Hunt* [2007] reported that $\tau = 0.7–1.4$ Pa was sufficient to prevent accumulation of Na- or Ca-montmorillonite in quartz sand, while *Bergendahl and Grasso* [2000] reported that a hydrodynamic shear of $\tau = 0.1$ Pa was sufficient to remove 50% of a monolayer of latex microspheres from glass beads. To put these stresses in context, *Tchobanoglous and Burton* [1991] reported $\tau = 0.03–0.15$ Pa for contact filtration, in which colloid aggregation proceeds within a sand filter. In this context, colloid mobilization is undesirable, so presumably this level of hydrodynamic shear is insufficient for colloid mobilization in contact filtration. In summary, shear stresses of 0.1–1 Pa appear to be sufficient to mobilize colloids in a wide range of systems. For a pore dimension of 100 μm, the implied fluid velocity is thus >0.01 m/s. Such values are comparable to flow-induced shear stresses in fractures generated by earthquakes in the intermediate to far field [*Brodsky et al.*, 2003]. Colloid mobilization by hydrodynamic shear is thus a plausible mechanism for some of the observed hydrological responses to earthquakes.

[46] The mechanical threshold is complicated by chemical conditions. Colloid mobilization generally occurs when the ionic strength (I) drops below the critical coagulation concentration, (CCC) [*Mays*, 2007]. The CCC, in turn, depends on the type of colloid, the pH, and the ratio of bivalent to monovalent cations, usually quantified using the sodium adsorption ratio (SAR). The effects of I, SAR, and pH can be represented using the Quirk-Schofield diagram [*Quirk and Schofield*, 1955], which plots the CCC as a function of

SAR for a given value of pH, such that chemical conditions favoring colloid dispersion are plotted below the line, and chemical conditions favoring colloid aggregation are plotted above the line (Figure 6). The influence of ionic strength on colloid mobilization (and associated effects on permeability), is then captured by the dimensionless ratio of ionic strength to critical coagulation concentration (I/CCC). If I/CCC < 1 dispersion results and if I/CCC > 1 aggregation results.

[47] Despite these complications, the experiments of *Roberts* [2005] discussed in section 3 illustrate how mechanical and chemical effects can be isolated by changing each independently. The experiments of *Roberts* [2005] suggest that physical and chemical effects on colloid mobilization and clogging can be usefully treated as independent variables.

[48] The abundance of mechanisms for colloid mobilization combined with the turbidity observations suggests that colloids may play a role in the hydrologic response of natural systems to transient stress. However, a critical question remains: Does breaking deposits increase permeability by opening the effective pore space, or decrease permeability by littering pore throats with newly mobilized colloids?

[49] To address this question, we distinguish between the behavior of natural porous media resembling *granular media filters*, which are essentially free of colloids, and those resembling *soils*, which contain a few percent colloids (by weight or volume). Natural porous media fall into both classes, but those resembling soils are more common—for example sandstones have a few percent clays, and their qualitative clogging behavior matches that of proper soils [*Mays*, 2010]. With this distinction, we can interpret observed relationships between colloid mobilization and permeability in steady flows, as illustrated in Figure 7. In granular media filters, for a given deposit, experiments conducted at slower flow rates or I/CCC > 1 cause more profound permeability reduction than otherwise identical experiments conducted at faster flow rates or I/CCC < 1. Slow flow and high ionic strength are both associated with deposits having smaller fractal dimensions [*Mays*, 2010]. The relationships between physicochemical changes and permeability are generally opposite in soils, where more profound permeability reduction is associated with fast flow and I/CCC < 1, which are both associated with deposits having larger fractal dimension [*Mays*, 2010]. Further work is needed to understand how transient flows change permeability in each case shown in Figure 7.

4.1.2. Mobilization of Drops and Bubbles

[50] The flow of two immiscible fluids, one wetting and one nonwetting, is common in natural hydrologic systems. It can occur, for example, in petroleum reservoirs and aquifers, and in both cases the wetting phase is typically water. In petroleum reservoirs, oil or natural gas constitutes the nonwetting phase, and, in aquifers, gas bubbles. The nonwetting phase at low-volume fractions tends to exist as a population of discrete droplets or bubbles (hereafter collectively called "droplets") dispersed in the wetting phase. Since the interface separating the phases has finite interfacial tension σ, and natural pores have small diameters, capillary forces affect flow.

a)   high fractal dimension   b) low fractal dimension

granular media filters

c)   d)
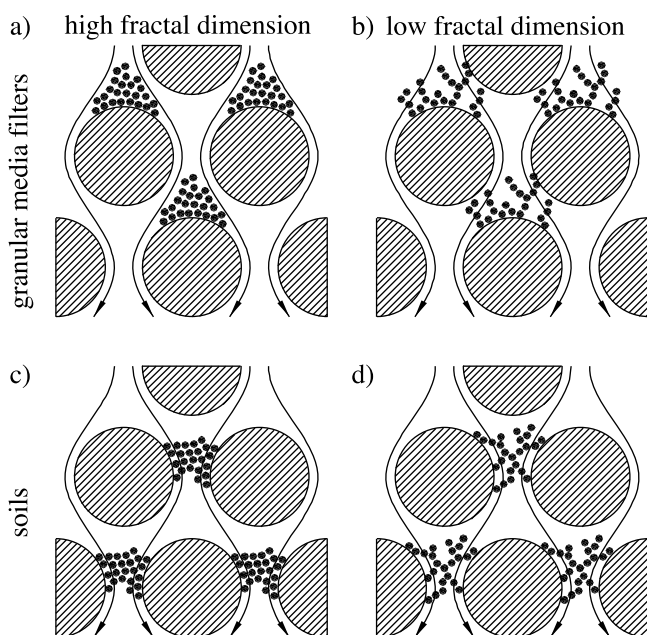
soils

Figure 7. Conceptual model linking colloid deposit morphology and permeability, distinguishing clean porous media (like *granular media filters*) in which particles can accumulate versus natural porous media (like *soils*) containing a few percent colloids and distinguishing more dendritic, low-fractal dimension deposits versus more compact, high-fractal dimension deposits. The number of particles shown is not representative of the particle concentration—soils have much higher concentrations. Each subplot has an identical number of deposited colloids. This conceptual model highlights the complex relationship between colloid mobilization and permeability. Reproduced from *Mays* [2010], with permission from the American Society of Civil Engineers.

[51] The presence of channel constrictions (radius r_{min}) between the larger pore bodies (radius r_{max}) is crucial for understanding the phenomenon of nonwetting-phase entrapment and hence disruption of the flow of the wetting fluid. Consider a droplet driven from left to right by an external pressure difference ΔP until the front meniscus starts to penetrate a narrow constriction (Figure 8). The positive mean curvatures of the left and right menisci are κ_{left} and κ_{right}. The pressures on the inner sides of the menisci are given by Laplace's law of capillary pressure. When these inner pressures become equal, the droplet is immobilized (trapped). The condition for the droplet to pass the constriction therefore is

$$\Delta P > \sigma\left(\kappa_{right} - \kappa_{left}\right). \qquad (4)$$

The entrapment of the nonwetting phase by capillary forces is known as the Jamin effect [*Taber*, 1969; *Melrose and Brandner*, 1974]. *Beresnev et al.* [2011] showed that the mobilization criterion (4) is accurate to within a few percent for oil droplets trapped in single constricted capillary.

[52] To understand how two-phase flow can be enhanced by elastic waves requires that we understand how vibrations

can overcome capillary entrapment. As proposed by *Graham and Higdon* [2000] and *Beresnev et al.* [2005], the mobilizing effect of vibrations can be understood by the following reasoning. The oil flow rate in straight pore channels obeys Darcy's law and is proportional to the external pressure gradient, equation (1). In a constricted channel, there is no flow until the external gradient exceeds a threshold value ∇P_{th} to overcome capillary entrapment. The vibration of the wall, induced by a passing seismic wave, is equivalent to the addition of an oscillatory "inertial" body force, with amplitude $F_{osc} = \rho A$, to the external gradient, where ρ is the density of the fluid and A is the amplitude of the acceleration of the wall [e.g., *Biot*, 1956]. When $\rho A_{mob} > \nabla P_{th} - \nabla P$, the droplet is unplugged; here A_{mob} is the "mobilizing" acceleration amplitude. Pushed forward over several vibrations, the droplet's leading meniscus may reach the neck of the constriction (with the radius r_{min} in Figure 8). Past that point, the resisting capillary force is reduced, the droplet is liberated, and flow is restored until the droplet is trapped at the next constriction.

[53] The amplitude of acceleration needed to mobilize the droplet is therefore

$$A_{mob} = (\nabla P_{th} - \nabla P)/\rho. \qquad (5)$$

Equation (5) is a "static" mobilization criterion, since it does not take into account the dynamics of motion of the droplet subjected to transient forces, and is thus the low-frequency limit. The higher the frequency, the shorter the "push" in the forward direction in a given period. To be mobilized, the droplet's leading meniscus must reach the neck of the constriction; the transport provided by a single oscillation is insufficient if the frequency is too high. The value of A_{mob} required to mobilize a given droplet is thus expected to grow as the wave frequency increases.

[54] A realistic fluid-saturated porous medium is characterized by a distribution of pore sizes and contains a certain concentration of trapped nonwetting phase with a distribution of droplet sizes. A seismic wave with given amplitude and frequency will mobilize a fraction of them. The fraction of mobilized droplets should increase with increasing amplitude and decreasing frequency of vibrations.

[55] *Beresnev et al.* [2005] and *Li et al.* [2005] reproduced the entrapment of a dispersed nonwetting phase in a lattice

droplet

r_{max}

$P+\Delta P$ $P+\Delta P+\sigma\kappa_{left}$ $P+\sigma\kappa_{right}$ r_{min} P

water
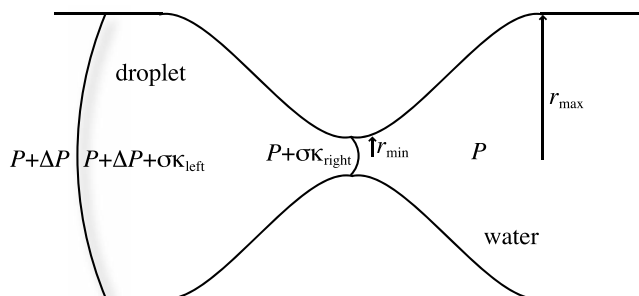
Figure 8. Geometry of trapped droplet defining length scales and pressures.
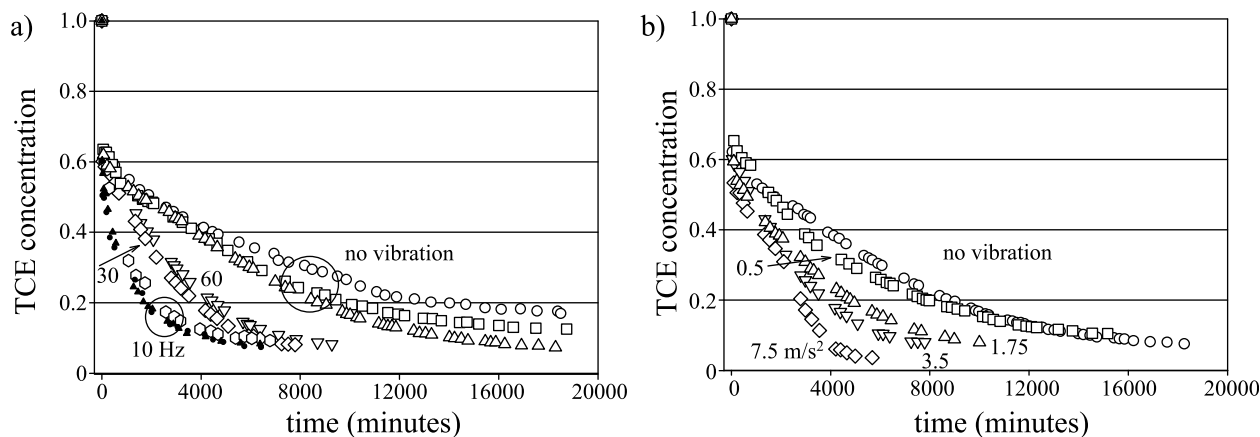
Figure 9. Concentration of nonwetting phase (TCE) as a function of time, demonstrating (a) the effect of frequency and (b) the effect of amplitude. The porous material here consists of a network of 50×50 circular pore bodies connected by straight throats etched onto a glass surface. The lattice was saturated with TCE which was then displaced until the residual saturation was reached. The upper three curves in Figure 9a and the upper curve in Figure 9b are control experiments with no vibrations. In Figure 9a the amplitude is fixed to 3.5 m/s^2 and frequencies are 10, 30 and 60 Hz. In Figure 9b the frequency is fixed to 30 Hz and amplitudes are 0.5, 1.75, 3.5, and 7.5 m/s^2. Modified from *Beresnev et al.* [2005].

of pore bodies connected by straight throats, etched on a horizontal glass surface. The lattice was saturated with an organic fluid, trichloroethylene (TCE), which was then flushed by water until an irreducible residual concentration of the entrapped fluid was reached. The experiments were first conducted without vibrations, and then with continuous in-plane vibrations at various amplitudes and frequencies. The residual concentrations were compared between the cases with and without vibration. Figure 9a shows that the nonwetting phase is removed faster (for fixed amplitude) as frequency decreases. Figure 9b confirms that during continuous stimulation, for a fixed frequency, the nonwetting phase is removed faster as the amplitude increases. For later comparison with observations and experiments, we need to convert accelerations, such as those in Figure 9, to strains. The strain in a plane seismic wave is v/c, where v is the amplitude of the particle velocity and c the wave propagation speed. For a wave with frequency f, using $v = A/(2\pi f)$, the seismic strain amplitude is $A/(2\pi fc)$.

[56] The static criterion does not describe the dynamics of mobilization nor the sensitivity to the frequency of vibrations. A more complete theory for mobilizing trapped droplets by seismic waves was developed by *Beresnev* [2006] and *Beresnev and Deng* [2010] in which a nonwetting droplet is represented as an oscillator driven by the balance of forces acting upon it. The resisting capillary force represents the restoring force of the oscillator. Writing Newton's second law for the balance of forces leads to an equation of motion for the droplet. In most situations, as expected, the dynamic theory is closer to the experimentally interpreted mobilization than the static criterion of equation (5) [*Beresnev et al.*, 2011].

[57] *Hilpert et al.* [2000] and *Hilpert* [2007] proposed that an oscillating droplet can be removed from its trapped configuration when driven at its resonance frequency. However, the theoretical model of *Beresnev* [2006] and *Beresnev and*

Deng [2010] suggests that the mobilization can be achieved at a continuum of frequencies, not only at resonance, as long as the leading meniscus is transported to the neck of the constriction. The resonance frequencies calculated from the two approaches [*Hilpert et al.*, 2000; *Beresnev*, 2006] are nearly identical [*Broadhead*, 2010].

[58] Many natural hydrologic systems are inherently two-phase fluid systems, containing a continuum of droplet sizes dispersed in suspending water. A subset of the continuum becomes immobilized in tortuous porous channels by capillary forces. The blocked channels reduce the bulk flow and the mobility of the two fluids, which is macroscopically seen as reduced permeability, a reduction in the term before ∇h in equation (1). The shallowest subsurface aquifers and soils may have gas bubbles, oil reservoirs clearly have dispersed droplets, and sedimentary basins may contain bubbles of natural gas. It is this ability to mobilize droplets that leads to the expectation that vibrations can enhance oil recovery and, as noted in the introduction, there is a long history of studying whether vibrations enhance oil recovery; field and laboratory studies show that stimulation can increase or decrease oil production, and the oil and gas industry remains largely skeptical of its value [e.g., *Roberts et al.*, 2003].

[59] The extent to which droplet mobilization by seismic waves plays a role in the natural observations summarized in section 2 is unclear. In fact, the storage properties of some aquifers that respond to earthquakes indicate that they do not have bubbles. A system containing a highly compressible phase will not respond sufficiently to dilatational strains to have a clear tidal or seismic response. Since tidal and seismic responses are observed in systems that also show permeability enhancement, bubbles cannot be invoked to explain the data from these wells [e.g., *Brodsky et al.*, 2003; *Elkhoury et al.*, 2006].

[60] The accelerations in natural hydrological systems that respond to earthquakes are as small as 10^{-4} m/s^2. Although

(a)

(b)
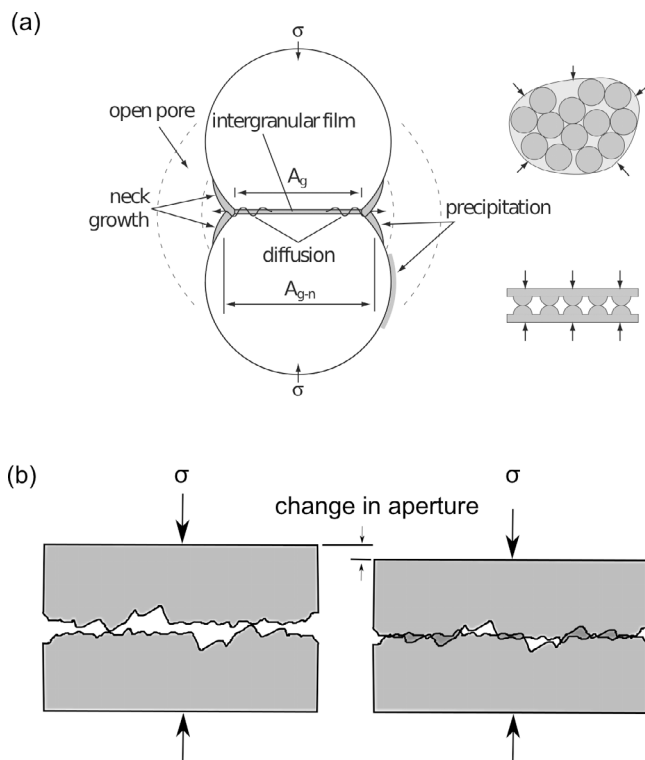
Figure 10. Mechanisms of pressure solution leading to fracture compaction. (a) Dissolution at point contacts promotes dissolution along the contacting surface and ejection to the pore space by diffusion along a water film [*Taron and Elsworth*, 2010]. Once in the pore space the dissolved mass may reprecipitate. (b) Where mineral mass is removed from contacting asperities the fracture will close despite net dissolution of solid mineral mass [*Yasuhara et al.*, 2004].

the accelerations and duration of shaking in Figure 9 are many orders of magnitude greater, the mobilization conditions are specific to the geometry of the porous material. The capillary mechanism in principle applies for all accelerations, at least during continuous stimulation, as a wave of a given particle acceleration and frequency can mobilize a certain subpopulation of the nonwetting droplets for which the mobilization criterion has been met.

4.2. Recovery of Permeability

[61] Some combination of mechanical and geochemical processes apparently causes enhanced permeability to return to approximately the prestimulated value. If permeability changed owing to the mobilization of particles and droplets, the recovery time scale may be controlled by the time to reclog pores or trap droplets. Here we consider one additional class of mechanical processes and then geochemical ones that operate on time scales of days to years, similar to those documented in Table 1. Geochemical processes may be relevant because the processes that govern recovery may be distinct from those that increase permeability—the field and laboratory observations show that permeability can change rapidly (seconds to minutes) but recovery can take years.

4.2.1. Poroelastic Processes

[62] Changes in permeability redistribute pore pressure, including pressures in the fractures that often dominate bulk permeability. *Faoro et al.* [2012] suggest that a slow recovery of permeability can be caused by depressurization of fractures. If the fluid pressure in the fracture increases coseismically, the mean aperture of the fracture increases, hence permeability increases. The gradual decrease in permeability occurs as pressure in the fracture diffuses into the matrix surrounding the fracture.

[63] The evolving permeability scales with the change in aperture Δb as $k/k_0 = (1 + \Delta b/b_0)^3$ where Δb is the change in aperture and b_0 is the initial aperture. Where mechanically soft fractures are embedded within an elastic medium, the permeability change scales with the cube of the amplitude of the pressure excursion (ΔP) as $k/k_0 = (1 + \alpha s \Delta P/b_0 E)^3$, where E is the elastic modulus, α is the Biot coefficient, and s is the spacing of fractures. When the coseismic pressure in the fracture increases an amount ΔP the bulk material experiences comparatively little increase in fluid pressure and net strain. This is an undrained response. Pore pressure will reequilibrate with that in the fracture, so that Δb will decrease in time at a rate that depends on the hydraulic diffusivity of the matrix and the fracture spacing. *Faoro et al.* [2012] document this permeability recovery experimentally and show that it agrees well with solutions to the coupled poroelastic and diffusion problems.

[64] For this mechanism to explain some of the field observations (section 2) and laboratory experiments (section 3), a large and sustained increase in fracture pressure is needed. How transient stresses might pressurize fractures is not clear, but changes in permeability do redistribute pore pressures, and fractures may be pressurized if hydraulic barriers are breached [*Sibson*, 1990]. This mechanism may be important for responses to large static stresses.

4.2.2. Permeability Recovery by Geochemical Processes

[65] Rocks can be pushed into chemical disequilibrium by changes in temperature, stress, fluid pressure, or invasion of new fluids. These are all processes that can be initiated by small transient stresses [*Moore et al.*, 1994; *Zhang et al.*, 1994; *Durham et al.*, 2001]. Disequilibrium can redistribute mineral matter through mechanisms of dissolution [*Gratier*, 1993; *Polak et al.*, 2003, 2004; *Detwiler*, 2008, 2010], transport [*Yasuhara et al.*, 2006], and precipitation that may both increase [*Polak et al.*, 2004; *Yasuhara et al.*, 2006] or decrease [*Polak et al.*, 2004; *Yasuhara et al.*, 2006] permeability. These effects can be especially strong in low-permeability fractured rocks where permeability is sensitive to small changes in the apertures of the constituent fractures and their connected pore networks. The rates of these effects are typically limited by kinetics or diffusive mass transport, rendering them incapable of explaining rapid coseismic changes in permeability. The time scales are, however, consistent with the slow rates of permeability recovery (Table 1) that extend over months to years. Laboratory measurements show that this resetting may occur over days at modest (80–150°C) temperatures [*Polak et al.*, 2003]
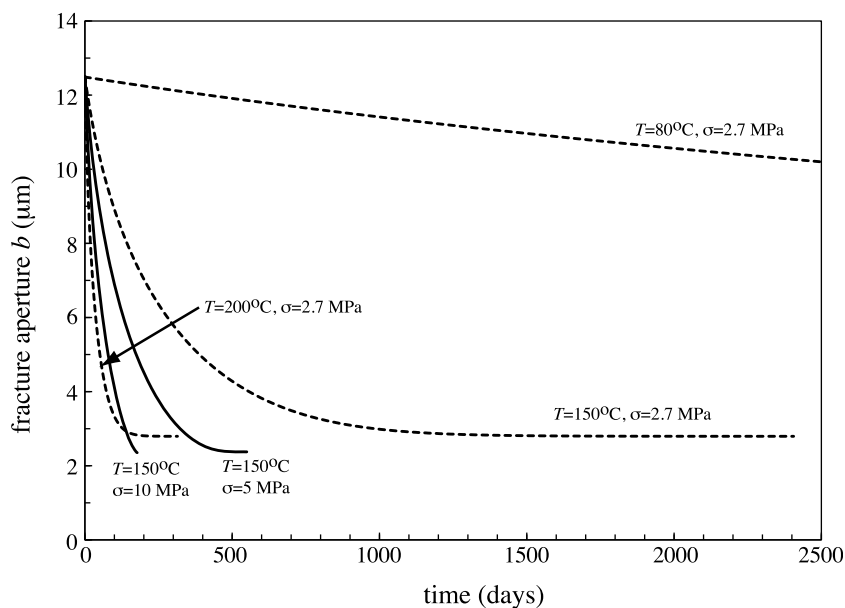
Figure 11. Rate of aperture closure for a fracture subjected to changes in temperature for constant stress (dashed) and for changes in stress at constant temperature (solid), based on data in *Yasuhara et al.* [2004].

and over months to years where temperatures are lower [*Yasuhara et al.*, 2004]. Fluid flow through experiments on fractures have revealed decreases in permeability of 1–2 orders of magnitude over tens of hours when there is net dissolution of the constituent solid minerals [e.g., *Polak et al.*, 2003; *Yasuhara et al.*, 2006]. These reductions are activated for modest changes in temperature [e.g., *Moore et al.*, 1994] or stress. Feasible mechanisms are stress-assisted dissolution [*Yasuhara et al.*, 2003, 2004; *Detwiler*, 2008], or stress-related subcritical crack growth and stress corrosion when temperatures are too low to invoke pressure solution [*Yasuhara and Elsworth*, 2008].

[66] The mechanisms of closure are illustrated in Figure 10 where stressed contacts elevate the potential at grain boundaries and promote dissolution. Dissolved mass is transported by diffusion within water films at grain boundaries and is ultimately released into the fluid-filled pore where it may reprecipitate. The transport rate typically slows with time as the driving mechanisms change: first, as the contacting asperity becomes wider, rates of mass transport drop as the diffusion path lengthens; second, the driving stress decreases as the contact area grows. Changes in the geometry of flow paths thus involve the three serial processes of (1) mineral mass dissolution, (2) mass diffusion, and (3) either mass precipitation or advection within the pore. The slowest of these processes represents the rate-controlling mechanism, and generally a numerical procedure is required to follow behavior even for relatively simple systems [e.g., *Taron and Elsworth*, 2010; *Detwiler*, 2010].

[67] An example of the effects of stress and temperature on fracture closure is shown in Figure 11 from the experiments reported in *Yasuhara et al.* [2004]. Under constant effective stress, the aperture approaches the same closure for all temperatures. This is expected since the asymptotic behavior is controlled by the dual parameters of critical

stress, σ_c, and equilibrium contact area. The critical stress is the stress required to initiate dissolution at a rate greater than that at the zero stress condition. As contact area grows the local stress ultimately decreases below the threshold stress required to induce mineral dissolution. Once dissolution is staunched, fracture closure effectively halts. This critical stress is only slightly influenced by system temperature, and contact area will evolve similarly for a given contact area–to–aperture relation for the fracture. In this case, the closure from 12 to 2 μm over the period of the observation results in a net reduction in permeability of over 2 orders of magnitude. For this particular case where precipitation has little influence on closure, the influence of temperature is larger than that of stress because the dissolution rate has an Arrhenius-type (exponential) dependence on temperature. Where effective stresses are increased at constant temperature, the rate dependence of closure is less pronounced. Doubling stress essentially doubles the closure rate, as anticipated because dissolution rate depends linearly on stress [*Yasuhara et al.*, 2004]. Lower-effective stresses result in slightly larger apertures. Rates of closure are in the range 10^{-13}–10^{-10} m/s. For tight (10 μm) and open (100 μm) fractures, the lower closure rates decrease permeability 65% and 10%, respectively, toward background within the period of a year—both feasible magnitudes to be consistent with permeability recovery rates observed in situ (section 2 and Table 1). These observations suggest that mechanical and geochemical interactions are both potential candidates to explain observations of permeability recovery in fractured reservoirs.

5. IMPLICATIONS FOR CRUSTAL PROCESSES

[68] Field observations in a wide range of geological settings (section 2) and laboratory experiments (sections 3
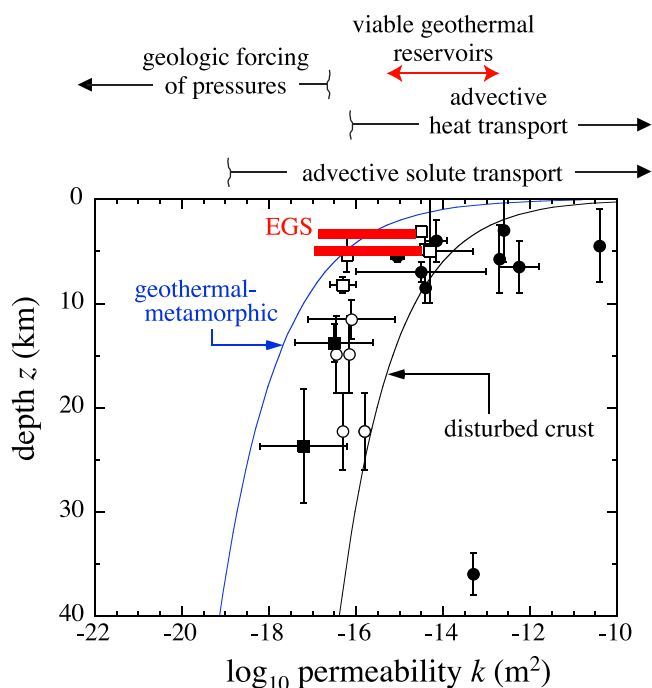
Figure 12. Evidence for relatively high crustal-scale permeabilities showing power law fit to data. Geothermal-metamorphic curve is the best fit to geothermal-metamorphic data [*Manning and Ingebritsen*, 1999; *Ingebritsen and Manning*, 2002]. "Disturbed-crust" curve interpolates midpoints in reported ranges in k and z for a given locality [*Ingebritsen and Manning*, 2010, Table 1]; error bars depict the full permissible range for a plotted locality and are not Gaussian errors, and the Dobi (Afar) earthquake swarm is not shown on this plot (it is offscale). Red lines indicate permeabilities before and after EGS reservoir stimulation at Soultz (upper line) and Basel (lower line) from *Evans et al.* [2005] and *Häring et al.* [2008], respectively. Arrows above the graph show the range of permeability in which different processes dominate.

and 4) show that transient stresses, with amplitudes as small as those generated by earthquakes at distances of a few fault lengths from the rupture, can change permeability and fluid pressure. Are these changes of any geological significance?

[69] Here we first put the magnitude of the permeability changes in context by comparing them with the permeability of the crust. We also consider whether the changes in permeability can feed back into tectonic processes, for example by triggering earthquakes.

5.1. Permeability of the Crust

[70] The permeability changes inferred from field observations (section 2) and documented in the lab (section 3) typically increase permeability a fewfold, with a few exceptions [e.g., *Geballe et al.*, 2011; *Wang et al.*, 2012]. To put these changes in context, we now compare such changes with those produced at the field scale by other natural geological processes and human intervention.

[71] Although permeability is heterogeneous, anisotropic, and varies over time, some order has been revealed in globally compiled data. Based on compilations of in situ

hydraulic test data, the mean permeability of crystalline rocks in the uppermost crust (<1 km depth) is approximately 10^{-14} m^2 [*Brace*, 1980; *Hsieh*, 1998], and decreases with depth [*Clauser*, 1992]. Direct in situ measurements of permeability are rare below depths of 2–3 km and nonexistent below 10 km. To complement direct measurements, geothermal data and estimates of fluid flux during prograde metamorphism have been used to constrain the permeability of regions of the continental crust undergoing active metamorphism and tectonism. A power law fit to these data yields

$$\log_{10}k \approx -14 - 3.2\log_{10}z, \qquad (6)$$

where k is in m^2 and z is in kilometers [*Manning and Ingebritsen*, 1999]. Equation (6) has been shown to be reasonably compatible with other independently compiled data [*Townend and Zoback*, 2000; *Shmonov et al.*, 2002, 2003; *Saar and Manga*, 2004; *Stober and Bucher*, 2007].

[72] The geothermal-metamorphic curve, equation (6), represents natural systems averaged over large spatial scales and long-time scales. Individual metamorphic permeability values are based on time-integrated fluid flux over the (generally long) time span of a metamorphic event. It has been suggested that lower permeabilities might be expected during metamorphism associated with cooling and decompression [*Yardley and Baumgartner*, 2007], or in the deep crust within stable cratons [*Ingebritsen and Manning*, 2002]. This suggestion is consistent with the fact that mean geothermal-metamorphic permeabilities are roughly 1 order of magnitude larger than mean "experimental" permeabilities [*Shmonov et al.*, 2003].

[73] On short time scales, permeability may reach values significantly in excess of those represented by equation (6). The evidence includes rapid migration of seismic hypocenters; enhanced rates of metamorphic reaction in major fault or shear zones; and recent studies suggesting much more rapid metamorphism than has been canonically assumed. Like the original compilation of geothermal-metamorphic permeabilities, Figure 12 shows that the high-permeability data suggest systematic variation with depth. A quantitative best fit to the data set as a whole yields

$$\log_{10}k \approx -11.7 - 2.9\log_{10}z, \qquad (7)$$

with k in m^2 and z in kilometers. This fit is obtained by grouping all of the "high-permeability" data given in Table 1 of *Ingebritsen and Manning* [2010].

[74] The sources of the disturbed crust data of Figure 12 include earthquake swarms that exhibit space-time progression consistent with triggering by propagation of an aqueous fluid pressure front. Earthquake triggering by propagation of an aqueous fluid pressure front can be initiated by sudden communication between a relatively high-pressure source and lower-pressure surroundings [e.g., *Miller et al.*, 2004; *Hill and Prejean*, 2005]. This suggests analogy with anthropogenic earthquake triggering by fluid injection [e.g., *Fischer et al.*, 2008; *Shapiro and Dinske*, 2009] and reservoir filling [*Talwani et al.*, 2007]. Studies of waste injection

at the Rocky Mountain Arsenal [*Hsieh and Bredehoeft*, 1981], the German Continental Deep Drilling Borehole (KTB), and the Soultz and Basel EGS sites have yielded particularly well-constrained hydraulic parameters. Note that the high permeability of disturbed crust, where k increases roughly 100-fold, is the result of shear or tensile failure, rather than the smaller transient stresses considered in the rest of this review.

[75] In geothermal resource exploration practice it has proven much easier to find sufficiently hot rock than to find sufficient permeability to support fluid production ($\sim$100 kg/s of hot water for commercially viable wells). Thus the EGS concept is to drill into hot rock and use hydraulic stimulation to create adequate reservoir permeability by creating thermoelastic stresses or pore pressure changes that lead to tensile or (more commonly) shear failure. EGS reservoir targets for electrical power generation are generally $\geq$3 km depth to reach adequate temperatures and require reservoir permeabilities $k \sim \geq 10^{-15}$ m^2 to permit adequate fluid flow rates (Figure 12) [*Björnsson and Bodvarsson*, 1990]. Equation (6) and other proposed permeability depth (k-z) curves suggest that $k \geq 10^{-15}$ m^2 will be unusual at $\geq$3 km depth, and in fact the initial, prestimulation permeabilities of the potential EGS reservoirs at Soultz and Basel were $k \sim 10^{-16.8}$ m^2 and $k \sim 10^{-17}$ m^2, too low to permit significant geothermal power production. Fluid injection at 2.85–3.45 km depth at Soultz and 4.6–5.0 km depth at Basel increased permeability >100-fold relative to prestimulation conditions [*Evans et al.*, 2005; *Häring et al.*, 2008]. These two EGS experiments shifted reservoir permeabilities from initial values compatible with what might be termed "geothermal-metamorphic crust" to values compatible with the "disturbed crust" (Figure 12). Poststimulation reservoir permeabilities at both Soultz and Basel were large enough to permit electrical power generation, $k \sim 10^{-14.5}$ m^2 at Soultz and $10^{-14.4}$ m^2 at Basel [*Evans et al.*, 2005; *Häring et al.*, 2008].

[76] The higher disturbed crust permeabilities depicted in Figure 12 must in general be localized and transient, perhaps occurring 2 or 3 orders of magnitude less often so that the time- and space-averaged permeability is much lower. If this were not the case, crustal heat transport would be advection dominated, and crustal temperatures would be generally lower than they are observed or inferred to be; large-scale crustal permeabilities greater than the approximate threshold for advective heat transport ($\sim 10^{-16}$ m^2 in the upper crust) must be relatively rare. Further, the high permeabilities depicted in Figure 12 would preclude the elevated fluid pressures that are believed to be pervasive below the brittle ductile transition, as overpressures typically require large regions of a flow domain (>100 m length scale) to be composed of, or bounded by, material with $k \leq 10^{-17}$ m^2 [*Neuzil*, 1995; *Manning and Ingebritsen*, 1999]. In the absence of active fluid sourcing and tectonism, permeability should tend to decrease due to processes such as mineral precipitation, hydrothermal alteration, and compaction (section 4.2.2). However, the rate of this decrease is poorly known. The time scales for permeability recovery after earthquakes and documented in the lab (Table 1) may provide a partial

guide for expected responses, but they may not be entirely relevant for recovery in crust disturbed by shear and tensile failure.

[77] If time scales for permeability recovery in EGS are similar to those in Table 1, months to years, then it may be necessary to somehow maintain permeability for economic viability and resource longevity. The largest geochemical disequilibria will be generated by the initial enhancement of permeability, and any subsequent small amplitude transient stresses should have a small effect on the recovery of permeability by geochemical processes (section 4.3.2). However, if flow paths are clogged by particles (precipitated minerals or preexisting fines), the experimental studies suggest that time-varying flows produced by transient stresses can mobilize trapped particles. Understanding how and why permeability decreases within the dominant flow paths in EGS will be a key to assessing whether imposing transient stresses, much smaller than those that created the fractures, can help maintain permeability.

5.2. Implications for Stimulated and Triggered Earthquakes

[78] The fact that permeability can change in response to transient stresses raises the possibility that hydromechanical coupling is an important part of the earthquake cycle, even in the intermediate and far field. Despite questions about mechanisms (sections 3 and 4), hydrological systems clearly respond to earthquakes (section 2). Faults are also hydrological systems which guide and store fluids in the crust. Pore pressure plays an important role in determining the frictional stability of faults and creating hydrofractures. Therefore, is it possible that earthquakes can affect distant fault zones through the intermediary of permeability enhancement by transient stresses? Interactions between seismicity on widely separated faults are commonly observed and linked to seismic waves [*Hill et al.*, 1993; *Gomberg et al.*, 2001; *West et al.*, 2005; *Felzer and Brodsky*, 2006; *Hill and Prejean*, 2007; *van der Elst and Brodsky*, 2010]. A key question is: what role, if any, does permeability enhancement play in promoting seismicity?

[79] A fault zone is a complex hydrogeological system that often consists of a low-permeability fault core embedded in a high-permeability, fracture-dominated damage zone [*Caine et al.*, 1996]. Faults are also notable for strongly compartmentalized fluids [*Zoback*, 2007]. Changing permeability can thus result in local pore pressure changes [*Brodsky et al.*, 2003] and changing pore pressure in a fault zone is one of the most effective ways known to trigger earthquakes [*Raleigh et al.*, 1976]. As pore pressure increases, the effective normal stress locking the fault decreases and therefore increases propensity for failure [*Hubbert and Rubey*, 1959]. Reservoir-induced seismicity with a time lag between impoundment and seismicity may be another example [e.g., *Talwani and Acree*, 1985; *Gupta*, 2002; *Ge et al.*, 2009]. It is thus expected on physical grounds that there should be a relationship between permeability enhancement and earthquake generation.
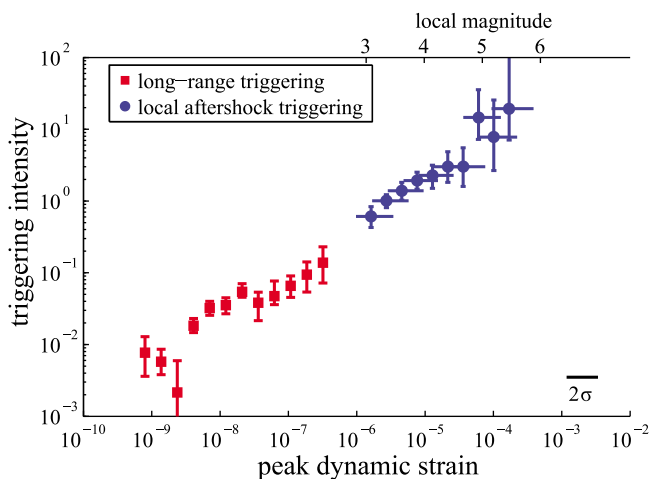
Figure 13. Seismicity rate change as a function of peak strain of seismic waves impacting the region (adapted from *van der Elst and Brodsky* [2010]).

[80] Recent work on earthquakes naturally triggered by seismic waves has shown that seismicity rate changes vary continuously with the magnitude of the perturbing stresses (Figure 13) [*van der Elst and Brodsky*, 2010]. Natural perturbations with stresses on the order 10^{-4}–1 MPa can trigger seismicity [*van der Elst and Brodsky*, 2010] and anthropogenic perturbations of 0.01–10 MPa have been linked to seismicity [*McGarr et al.*, 2002]. The continuous nature of permeability enhancement by time-varying stresses (Figure 5) suggests a mechanism that is consistent with this observation. However, such connections have not been directly observed and are still quite speculative. Some of the most important observational gaps are (1) direct observations of permeability changes at depth in and near a fault zone, (2) direct connection between permeability changes and effective stress changes in a fault zone, and (3) quantification of the degree of permeability enhancement in a region of triggered seismicity.

6. SUMMARY AND OPEN QUESTIONS

[81] Field observations and laboratory experiments show that oscillatory stresses, such as those created by natural earthquakes or artificial vibrations, can change permeability k or fluid mobility (the term in front of ∇h in equation (1)). The laboratory experiments reviewed in section 3 and mechanisms discussed in section 4 provide a framework for trying to understand the response of natural and engineered systems to transient stresses such as those generated by earthquakes. Connecting any specific field-scale observation to a mechanism remains challenging because the subsurface cannot be easily monitored at the pore scale where mechanisms operate. However, the following observations may be useful for distinguishing among the various mechanisms.

[82] First, *Brodsky et al.* [2003] found that some earthquake-induced sustained water level changes in wells were preceded by water level oscillations with progressively increasing amplitude prior to the sustained water level change. This observation, combined with the experimental observation that permeability changes scale with the amplitude of forcing (Figure 5), suggests that the sustained water level change develops progressively by oscillatory flow and that there may be a threshold for changing permeability. These observations are more consistent with mobilization of trapped colloidal particles or droplets which are progressively mobilized beyond some threshold, than with poroelastic opening or closing of fractures. Second, the common occurrence of turbidity in wells is consistent with mobilization of colloidal particles in pores and fractures of aquifers. Third, there are large differences in the minimum seismic energy for various earthquake-induced hydrological responses. For example, the threshold seismic energy density for liquefaction of soils, changes in stream discharge, and the eruption of mud volcanoes is $e \sim 10^{-1}$ J/m^3 (Figure 1), while that for changing groundwater level and temperature is only $e \sim 10^{-4}$ J/m^3 [*Wang and Manga*, 2010a]. Regardless of whether the mechanism for hydrological responses is directly connected to seismic energy density, these differences imply very different sensitivities to transient stresses. While part of this difference may be due to incomplete data, some data sets, such as those for groundwater level and liquefaction, are extensive, and the differences in the threshold seismic energy density should be robust. These differences indicate that there may be more than one mechanism at work and that different mechanisms may be responsible for different hydrological responses.

[83] Figure 14 summarizes strain amplitudes and permeability changes for the lab experiments reviewed in sections 3 and 4 and for field observations for which permeability changes were explicitly quantified and reported. For the bubble mobilization experiments of *Beresnev et al.* [2005] and *Li et al.* [2005] we assumed a wave velocity of 3 km/s. We can draw a few conclusions from this compilation: first, permeability usually increases; second, strain amplitudes as small as 10^{-6} can change permeability; third, permeability generally increases by less than a factor of ten unless new fractures form or their width increases significantly owing to pressurization of fractures (section 4.2.1). The observations in Figure 14 are subdivided by frequency, with filled boxes indicating frequencies greater than or equal to 10 Hz; everything else, except *Faoro et al.* [2012], has frequencies between 0.05 and 10 Hz, the range of seismic frequencies that cause the field responses described in section 2. A frequency dependence is not obvious, but we emphasize that more experiments and observations are needed.

[84] In the introduction we listed several open questions that are relevant for understanding observations of natural systems and for using stimulation to modulate and maintain permeability in engineered systems. To summarize, we revisit those questions and our current state of understanding.

[85] 1. What are possible pore- and fracture-scale mechanisms for permeability changes? Are new pathways being created? Or, are existing paths being unclogged?
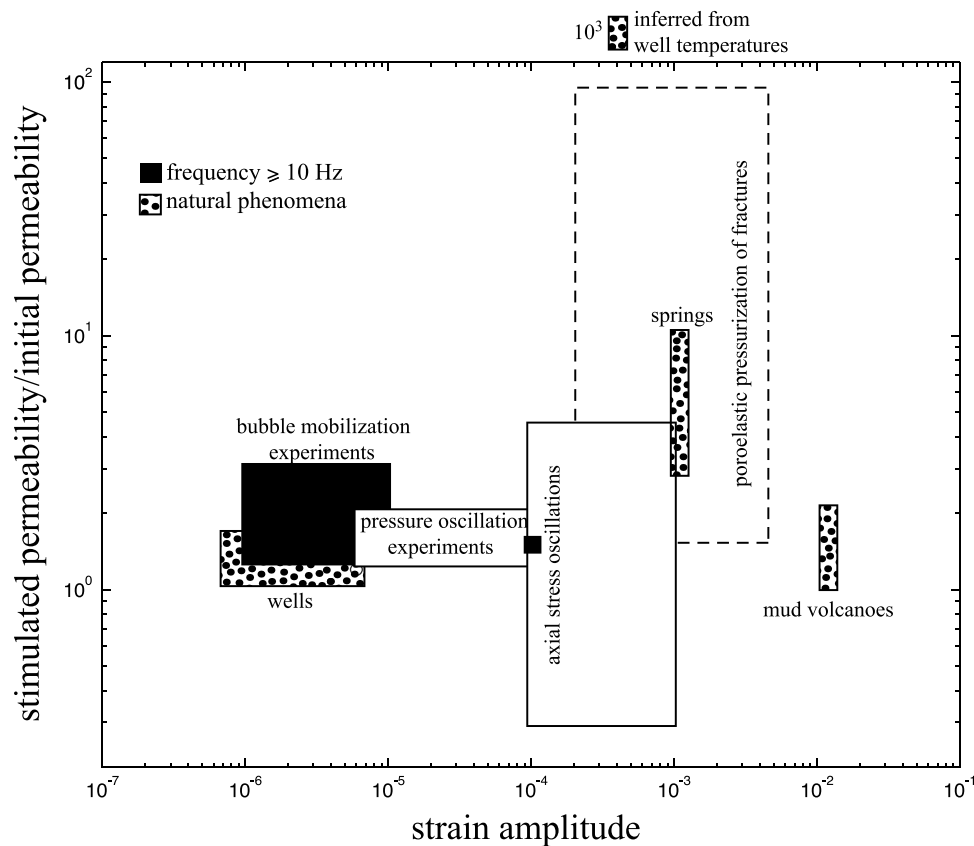
Figure 14. Summary of the permeability changes documented in the lab and field as a function of strain amplitude. Stippled boxes indicate field observations. Black filled boxes indicate experiments with frequencies ≥10 Hz. The dashed box indicates the strain amplitude and permeability changes for the pressurized fracture experiments presented in *Faoro et al.* [2012]—these are the only responses to nonoscillatory deformation shown in the compilation. Sources are as follows: bubble mobilization experiments [*Li et al.*, 2005]; pressure oscillation experiments [*Elkhoury et al.*, 2011]; axial stress oscillations in black [*Roberts*, 2005] and in white [*Liu and Manga*, 2009; *Shmonov et al.*, 1999]; well temperatures [*Wang et al.*, 2012], with strain from *Koizumi et al.* [2004]; springs [*Manga and Rowland*, 2009]; mud volcanoes [*Rudolph and Manga*, 2010]; wells [*Elkhoury et al.*, 2006].

[86] The mechanism or mechanisms by which these changes occur in any particular case remain uncertain, and in natural settings may be impossible to determine because of the complexity and inaccessibility of the subsurface. The mechanisms reviewed in section 4 are all substantiated by experimental studies, so in principle all may be relevant for natural settings and engineered systems. Given that the seismic stresses are too small to create new pathways mechanically, e.g., by fracturing, and that permeability changes occur too fast to be consistent with new pathways created geochemically, e.g., by dissolution, it is most likely that existing pathways are being cleared or unblocked. More work is needed to understand the physicochemical processes that mobilize colloids and nonwetting phases in transient flows. The possible role of permeability changes in aquifers on the occurrence of liquefaction deserves further study; if there is a connection, there are implications for hazard assessment.

[87] 2. Is there a frequency dependence?

[88] That is, for the same strain or vibration amplitude, is there a dependence on the frequency of the oscillations?

Manga et al. [2009] find a possible frequency dependence for the triggered eruption of mud volcanoes, with a greater sensitivity to long-period waves. There is conflict between results for liquefaction, with little frequency dependence found in the lab [*Yoshimi and Oh-Oka*, 1975; *Sumita and Manga*, 2008], but liquefaction in the field appears to be favored by low-frequency ground motion [*Wang et al.*, 2003; *Youd and Carter*, 2005; *Holzer and Youd*, 2007; *Wong and Wang*, 2007]. Triggered seismicity appears to be more sensitive to long-period waves than short-period ones of comparable amplitude [*Brodsky and Prejean*, 2005]. This observation might favor permeability enhancement being part of the triggering process, as the diffusive flow forcing water into a fault from the adjoining porous medium is a low-pass filter. For fixed acceleration amplitude, mobilization of droplets is enhanced at low frequencies (section 4.1.2). Therefore, the current evidence favors long-period waves as being more effective at increasing permeability at a given amplitude than short-period ones. Engineered permeability enhancement systems might thus benefit from focusing on

long-period waves. However, the data supporting this preliminary conclusion are still extremely sparse.

[89] 3. Does permeability always increase?

[90] In most natural systems permeability appears to increase after earthquakes. This is also true in laboratory experiments. There are a few cases of decreases such as the lab experiments of *Shmonov et al.* [1999] and *Liu and Manga* [2009] but the reductions are small. The magnitude of permeability changes caused by transient stresses, typically factors of a few, is much smaller than the changes caused by shear failure and hydrofracture that can increase permeability by a couple orders of magnitude (Figures 12 and 14).

[91] The relationship between the magnitude of transient stresses and the magnitude of responses is unclear. Laboratory studies (Figure 5) and some field observations [*Manga et al.*, 2003; *Elkhoury et al.*, 2006] show that the magnitudes of water level or discharge changes scale with the magnitude of stresses. This scaling is contradicted by other observations [*King et al.*, 1994; *Manga and Rowland*, 2009] that suggest that the magnitude of responses, when they occur, are always similar, implying changes in permeability of fixed magnitude once a threshold is exceeded. More examples are needed to document how given systems respond to multiple earthquakes or stimulations.

[92] 4. Dynamically increased permeability seems to return to its prestimulated value. What controls the recovery time?

[93] At the field scale, permeability recovers on time scales of minutes to years (Table 1). There are likely to be observational biases at both ends of this range. Nevertheless many months to a few years seems to be the most common time scale. Geochemical processes to reduce permeability are effective on similar time scales (section 4.2). If this is the primary mechanism, the rate is controlled mainly by the extent of disequilibrium (new fluid sources, mixing of fluids) and temperature. Shallow cold systems should take longer to return to prestimulation values. Existing observations are not extensive enough to recognize a temperature control on recovery in natural systems.

[94] When droplets or colloidal particles are mobilized, the recovery time is determined by the time for trapping droplets or creating new colloidal deposits. For droplets, this time would be the time for droplets to move to the next constriction. For a flow rate of ~1 m d^{-1} and a distance between trapping constrictions of 1 mm, the recovery time would be short, 1 min. Owing to the feedback between trapping and flow, however, flow fluctuations caused by mobilization are amplified. This can hinder trapping to some extent, but the time scale will still be short [*Hunt and Manga*, 2003]. If the wave stimulation is prolonged, bubbles and droplets may move continuously through a series of constrictions until the wave excitation stops. For colloidal particles the recovery time may be much longer as it may require transport of particles over longer distances and changes in water chemistry. With both processes, the recovery time is controlled by pore geometries and flow rates.

[95] 5. What materials are the most sensitive? Is there a threshold for hydrologic response in terms of strain amplitude or hydrodynamic shear?

[96] The observational database (Figure 1) and laboratory experiments are not complete and systematic enough to identify patterns and trends. The experimental studies, however, suggest that the presence of mobile particles, drops, and bubbles will increase the susceptibility to permeability enhancement. Tight rocks such as shales and fractured crystalline rocks should also be susceptible, because small changes in the geometry of flow paths and unblocking fractures will have a large effect on permeability. The data in Figure 5, however, do not support this expectation for sandstones, and additional measurements are needed for low-permeability rocks. It remains unclear whether there is a strain amplitude threshold for changing permeability, as implied by the compilation of natural observations in Figure 1; none is necessary for mobilization of a dispersed droplet phase, for example (section 4). The limited studies of hydrodynamic shear summarized in this review suggest that there may be a critical shear stress (at the pore scale) for colloid mobilization, in the range of 0.1–1 Pa. However, that may be an apparent threshold in that the consequences of permeability changes must be large enough to be detectable. If permeability enhancement scales with the magnitude of strains (e.g., Figure 5) the threshold in Figure 1 may indicate the limit of being able to detect changes. Triggered seismicity appears to have no such thresholds (Figure 13).

[97] 6. Can dynamic stresses be used to maintain permeability in enhanced geothermal systems? Can monitoring of productive geothermal systems provide insight into permeability evolution?

[98] Stimulation by transient stresses, much smaller than those that hydrofracture rock or cause shear failure, may be able to maintain permeability if the dominant permeability reduction mechanism is the clogging of flow paths by a dispersed phase such as colloidal particles. Identifying permeability reduction mechanisms is thus the starting point for assessing whether stimulation will be useful in EGS or other engineered geological systems.

[99] Monitoring permeability evolution in regions with artificially enhanced permeability provides opportunities to understand how and why permeability is influenced by external processes, such as stress from earthquakes, and to evaluate permeability recovery mechanisms. The connection between permeability enhancement and seismicity may be most effectively studied in regions where significant hydrogeological control is available and seismicity is abundantly generated. Candidate regions include geothermal facilities, which are known to stimulate significant seismicity, although the mechanisms are often unclear [*Majer et al.*, 2007; *Shapiro et al.*, 2010]. Places such the Salton Sea geothermal system or The Geysers geothermal field provide excellent laboratories for monitoring field scale fluid flow and permeability changes in response to seismic waves and connecting the behavior to the ensuing sequence of further earthquakes.

[100] In summary, it is now clear that transient stresses can change permeability and the mobility of fluids in porous materials. The mechanisms responsible for such changes, however, remain unclear. Continued monitoring of the responses to earthquakes, controlled laboratory studies, and targeted field projects at the scale of subsurface engineered systems may provide insight into how transient stress influences permeability. Understanding the connection between stress and permeability is fundamental to understanding the interaction between tectonics and hydrogeology, and the stresses generated by earthquakes and other transient stresses provide opportunities to probe the underlying physicochemical processes.

REFERENCES

Ambraseys, N. N. (1988), Engineering seismology, *Earthquake Eng. Struct. Dyn.*, *17*, 1–50, doi:10.1002/eqe.4290170101.

Backhus, D. A., J. N. Ryan, D. M. Groher, J. K. MacFarlane, and P. M. Gschwend (1993), Sampling colloids and colloid-associated contaminants in ground water, *Ground Water*, *31*, 466–479, doi:10.1111/j.1745-6584.1993.tb01849.x.

Bai, R., and C. Tien (1997), Particle detachment in deep bed filtration, *J. Colloid Interface Sci.*, *186*, 307–317, doi:10.1006/jcis.1996.4663.

Beckham, R., A. I. Abdel-Fattah, P. M. Roberts, S. Tarimala, and R. H. Ibrahim (2010), Mobilization of colloidal particles by low-frequency dynamic stress stimulation, *Langmuir*, *26*(1), 19–27, doi:10.1021/la900890n.

Beresnev, I. A. (2006), Theory of vibratory mobilization of nonwetting fluids entrapped in pore constrictions, *Geophysics*, *71*, 47–56.

Beresnev, I. A., and W. Deng (2010), Viscosity effects in vibratory mobilization of residual oil, *Geophysics*, *75*, N79–N85.

Beresnev, I. A., and P. A. Johnson (1994), Elastic-wave stimulation of oil production: A review of methods and results, *Geophysics*, *59*, 1000–1017, doi:10.1190/1.1443645.

Beresnev, I. A., R. D. Vigil, W. Li, W. D. Pennington, R. M. Turpening, P. P. Iassonov, and R. P. Ewing (2005), Elastic waves push organic fluids from reservoir rock, *Geophys. Res. Lett.*, *32*, L13303, doi:10.1029/2005GL023123.

Beresnev, I. A., W. Gaul, and R. D. Vigil (2011), Direct pore-level observation of permeability increase in two-phase flow by shaking, *Geophys. Res. Lett.*, *38*, L20302, doi:10.1029/2011GL048840.

Bergendahl, J., and D. Grasso (2000), Prediction of colloid detachment in a model porous media: Hydrodynamics, *Chem. Eng. Sci.*, *55*, 1523–1532, doi:10.1016/S0009-2509(99)00422-4.

Biagi, P. F., L. Castellana, A. Minafra, G. Maggipinto, A. Ermini, O. Molchanov, Y. M. Khatevich, and E. I. Gordeev (2006), Groundwater chemical anomalies connected with the Kamchatka earthquake (M = 7.1) on March 1992, *Nat. Hazards Earth Syst. Sci.*, *6*, 853–859, doi:10.5194/nhess-6-853-2006.

Biot, M. A. (1956), Theory of propagation of elastic waves in a fluid-saturated porous solid. II. Higher frequency range, *J. Acoust. Soc. Am.*, *28*, 179–191, doi:10.1121/1.1908241.

Björnsson, G., and G. Bodvarsson (1990), A survey of geothermal reservoir properties, *Geothermics*, *19*, 17–27, doi:10.1016/0375-6505(90)90063-H.

Borg, I. Y., R. Stone, H. B. Levy, and L. D. Ramspott (1976), Information pertinent to the migration of radionuclides in ground water at the Nevada Test Site: Part 2: Annotated bibliography, *Rep. UCRL-52078*, Lawrence Livermore Natl. Lab., Livermore, Calif.

Brace, W. F. (1980), Permeability of crystalline and argillaceous rocks, *Int. J. Rock Mech. Min. Sci. Geomech. Abstr.*, *17*, 241–251, doi:10.1016/0148-9062(80)90807-4.

Briggs, R. O. (1991), Effects of Loma Prieta earthquake on surface waters in Waddel Valley, *Water Resour. Bull.*, *27*, 991–999, doi:10.1111/j.1752-1688.1991.tb03148.x.

Broadhead, M. K. (2010), Oscillating oil drops, resonant frequencies, and low-frequency passive seismology, *Geophysics*, *75*, 1–8, doi:10.1190/1.3280041.

Brodsky, E. E., and S. G. Prejean (2005), New constraints on mechanisms of remotely triggered seismicity at Long Valley Caldera, *J. Geophys. Res.*, *110*, B04302, doi:10.1029/2004JB003211.

Brodsky, E. E., E. Roeloffs, D. Woodcock, I. Gall, and M. Manga (2003), A mechanism for sustained groundwater pressure changes induced by distant earthquakes, *J. Geophys. Res.*, *108*(B8), 2390, doi:10.1029/2002JB002321.

Caine, J. S., J. P. Evans, and C. B. Forster (1996), Fault zone architecture and permeability structure, *Geology*, *24*, 1025–1028, doi:10.1130/0091-7613(1996)024<1025:FZAAPS>2.3.CO;2.

Cappa, F., J. Rutqvist, and K. Yamamoto (2009), Modeling crustal deformation and rupture processes related to upwelling of deep CO_2-rich fluids during the 1965–1967 Matsushiro earthquake swarm in Japan, *J. Geophys. Res.*, *114*, B10304, doi:10.1029/2009JB006398.

China Earthquake Administration (1976), *China Earthquake Catalog*, 500 pp., Cent. for Chin. Res. Mater., Washington, D. C.

Claesson, L., A. Skelton, C. Graham, C. Dietl, M. Mörth, P. Torssander, and I. Kockum (2004), Hydrogeochemical changes before and after a major earthquake, *Geology*, *32*, 641–644, doi:10.1130/G20542.1.

Claesson, L., A. Skelton, C. Graham, and C.-M. Morth (2007), The timescale and mechanisms of fault sealing and water-rock interaction after an earthquake, *Geofluids*, *7*, 427–440, doi:10.1111/j.1468-8123.2007.00197.x.

Clauser, C. (1992), Permeability of crystalline rocks, *Eos Trans. AGU*, *73*(21), 233, doi:10.1029/91EO00190.

Cleasby, J. L., M. M. Williamson, and E. R. Baumann (1963), Effect of filtration rate changes on quality, *J. Am. Water Works Assoc.*, *55*, 869–877.

Coble, R. W. (1965), The effects of the Alaskan earthquake of March 27, 1964 on ground water in Iowa, *Proc. Iowa Acad. Sci.*, *72*, 323–332.

Cooper, H. H., J. D. Bredhoeft, I. S. Papdopulos, and R. R. Bennett (1965), The response of well-aquifer systems to seismic waves, *J. Geophys. Res.*, *70*, 3915–3926, doi:10.1029/JZ070i016p03915.

Cox, S. C., H. J. Rutter, A. Sims, T. W. Horton, M. Manga, T. Ezzy, J. J. Weir, and D. Scott (2012), Hydrological effects of the Darfield (Canterbury) M_w 7.1 earthquake, 4 September 2010, New Zealand, *N. Z. J. Geol. Geophys.*, in press.

Davis, E. E., K. Wang, R. E. Thomson, K. Becker, and J. F. Cassidy (2001), An episode of seafloor spreading and associated plate

deformation inferred from crustal fluid pressure transients, *J. Geophys. Res.*, *106*, 21,953–21,963, doi:10.1029/2000JB000040.

Detwiler, R. L. (2008), Experimental observations of deformation caused by mineral dissolution in variable-aperture fractures, *J. Geophys. Res.*, *113*, B08202, doi:10.1029/2008JB005697.

Detwiler, R. L. (2010), Permeability alteration due to mineral dissolution in partially saturated fractures, *J. Geophys. Res.*, *115*, B09210, doi:10.1029/2009JB007206.

Durham, W. B., W. L. Bourcier, and E. A. Burton (2001), Direct observation of reactive flow in a single fracture, *Water Resour. Res.*, *37*, 1–12, doi:10.1029/2000WR900228.

Dziak, R. P., W. W. Chadwick, G. G. Fox, and R. W. Embley (2003), Hydrothermal temperature changes at the southern Juan de Fuca Ridge associated with M_w 6.2 Blanc transform earthquake, *Geology*, *31*, 119–122, doi:10.1130/0091-7613(2003)031<0119:HTCATS>2.0.CO;2.

Elkhoury, J. E., E. E. Brodsky, and D. C. Agnew (2006), Seismic waves increase permeability, *Nature*, *441*, 1135–1138, doi:10.1038/nature04798.

Elkhoury, J. E., A. Niemeijer, E. E. Brodsky, and C. Marone (2011), Laboratory observations of permeability enhancement by fluid pressure oscillation of in-situ fractured rock, *J. Geophys. Res.*, *116*, B02311, doi:10.1029/2010JB007759.

Evans, K. F., A. Genter, and J. Sausss (2005), Permeability creation and damage due to massive fluid injections into granite at 3.5 km at Soultz: 1. Borehole observations, *J. Geophys. Res.*, *110*, B04203, doi:10.1029/2004JB003168.

Faoro, I., D. Elsworth, and C. Marone (2012), Permeability evolution during dynamic stressing of dual permeability media, *J. Geophys. Res.*, *117*, B01310, doi:10.1029/2011JB008635.

Felzer, K. R., and E. E. Brodsky (2006), Decay of aftershock density with distance indicates triggering by dynamic stress, *Nature*, *441*, 735–738, doi:10.1038/nature04799.

Fischer, T., S. Hainzl, L. Eisner, S. A. Shapiro, and J. Le Calvez (2008), Microseismic signatures of hydraulic fracture growth in sediment formations: Observations and modeling, *J. Geophys. Res.*, *113*, B02307, doi:10.1029/2007JB005070.

Galli, P. (2000), New empirical relationships between magnitude and distance for liquefaction, *Tectonophysics*, *324*, 169–187, doi:10.1016/S0040-1951(00)00118-9.

Gao, B., J. E. Saiers, and J. N. Ryan (2004), Deposition and mobilization of clay colloids in unsaturated porous media, *Water Resour. Res.*, *40*, W08602, doi:10.1029/2004WR003189.

Ge, S., M. Liu, N. Lu, L. W. Godt, and G. Luo (2009), Did the Zipingpu Reservoir trigger the 2008 Wenchuan earthquake?, *Geophys. Res. Lett.*, *36*, L20315, doi:10.1029/2009GL040349.

Geballe, Z. M., C.-Y. Wang, and M. Manga (2011), A permeability-change model for water level changes triggered by teleseismic waves, *Geofluids*, *11*, 302–308, doi:10.1111/j.1468-8123.2011.00341.x.

Gibs, J., Z. Szabo, T. Ivahnenko, and F. D. Wilde (2000), Change in field turbidity and trace element concentrations during well purging, *Ground Water*, *38*, 577–588, doi:10.1111/j.1745-6584.2000.tb00250.x.

Glasgow, G. D. E., and A. D. Wheatley (1998), The effect of surges on the performance of rapid gravity filtration, *Water Sci. Technol.*, *37*, 75–81, doi:10.1016/S0273-1223(98)00012-2.

Gleeson, T., L. Marklund, L. Smith, and A. H. Manning (2011), Classifying the water table at regional to continental scales, *Geophys. Res. Lett.*, *38*, L05401, doi:10.1029/2010GL046427.

Gomberg, J., et al. (2001), Earthquake triggering by seismic waves following the Landers and Hector Mine earthquakes, *Nature*, *411*, 462–466, doi:10.1038/35078053.

Graham, D. R., and J. J. L. Higdon (2000), Oscillatory flow of droplets in capillary tubes. Part 2. Constricted tubes, *J. Fluid Mech.*, *425*, 55–77, doi:10.1017/S0022112000002032.

Gratier, J. P. (1993), Experimental pressure solution of halite by an indenter technique, *Geophys. Res. Lett.*, *20*, 1647–1650, doi:10.1029/93GL01398.

Green, R. A., and J. K. Mitchell (2004), Energy-based evaluation and remediation of liquefiable soils, in *Geotechnical Engineering for Transportation Projects: Proceedings of Geo-Trans 2004, July 27–31, 2004, Los Angeles, California*, edited by M. K. Yegian and E. Kavazanjianpp, pp. 1961–1970, Am. Soc. of Civ. Eng., Reston, Va.

Gupta, H. K. (2002), A review of recent studies of triggered earthquakes by artificial water reservoirs with special emphasis on earthquakes in Koyna, India, *Earth Sci. Rev.*, *58*, 279–310, doi:10.1016/S0012-8252(02)00063-6.

Häring, M. O., U. Schanz, F. Ladner, and B. C. Dyer (2008), Characterisation of the Basel 1 enhanced geothermal system, *Geothermics*, *37*, 469–495, doi:10.1016/j.geothermics.2008.06.002.

Hill, D. P., and S. Prejean (2005), Magmatic unrest beneath Mammoth Mountain, California, *J. Volcanol. Geotherm. Res.*, *146*, 257–283, doi:10.1016/j.jvolgeores.2005.03.002.

Hill, D. P., and S. G. Prejean (2007), Dynamic triggering, in *Earthquake Seismology, Treatise on Geophysics*, edited by H. Kanamori, pp. 258–288, Elsevier, Amsterdam.

Hill, D. P., et al. (1993), Seismicity remotely triggered by the magnitude 7.3 Landers, California, earthquake, *Science*, *260*, 1617–1623, doi:10.1126/science.260.5114.1617.

Hilpert, M. (2007), Capillarity-induced resonance of blobs in porous media: Analytical solutions, Lattice-Boltzmann modeling, and blob mobilization, *J. Colloid Interface Sci.*, *309*, 493–504, doi:10.1016/j.jcis.2006.11.052.

Hilpert, M., G. H. Jirka, and E. J. Plate (2000), Capillarity-induced resonance of oil blobs in capillary tubes and porous media, *Geophysics*, *65*, 874–883, doi:10.1190/1.1444784.

Hochella, M. F., Jr., D. Aruguete, B. Kim, and A. S. Madden (2012), Naturally occurring inorganic nanoparticles: General assessment and a global budget for one of Earth's last unexplored geochemical components, in *Nature's Nanostructures*, edited by H. G. A. Barnard, pp. 1–42, Pan Stanford, Singapore.

Holzer, T. L., and T. L. Youd (2007), Liquefaction, ground oscillation, and soil deformation at the Wildlife Array, California, *Bull. Seismol. Soc. Am.*, *97*, 961–976, doi:10.1785/0120060156.

Holzer, T. L., J. C. Tinsley, and T. C. Hank (1989), Dynamics of liquefaction during the 1987 Superstition Hills, California, earthquake, *Science*, *244*, 56–59, doi:10.1126/science.244.4900.56.

Hsieh, P. A. (1998), Scale effects in fluid flow through fractured geologic media, in *Scale Dependence and Scale Invariance in Hydrology*, edited by G. Sposito, pp. 335–353, Cambridge Univ. Press, New York, doi:10.1017/CBO9780511551864.013.

Hsieh, P. A., and J. D. Bredehoeft (1981), A reservoir analysis of the Denver earthquakes: A case of induced seismicity, *J. Geophys. Res.*, *86*, 903–920, doi:10.1029/JB086iB02p00903.

Hubbert, M. K., and W. Rubey (1959), Role of fluid pressure in mechanics of overthrust faulting, *Geol. Soc. Am. Bull.*, *70*, 115–205, doi:10.1130/0016-7606(1959)70[115:ROFPIM]2.0.CO;2.

Hunt, A. G., and M. Manga (2003), Effects of bubbles on the hydraulic conductivity of porous materials–Theoretical results, *Transp. Porous Media*, *52*, 51–65, doi:10.1023/A:1022312927606.

Ingebritsen, S. E., and C. E. Manning (2002), Diffuse fluid flux through orogenic belts: Implications for the world ocean, *Proc. Natl. Acad. Sci. U. S. A.*, *99*, 9113–9116, doi:10.1073/pnas.132275699.

Ingebritsen, S. E., and C. E. Manning (2010), Permeability of the continental crust: Dynamic variations inferred from seismicity and metamorphism, *Geofluids*, *10*, 193–205.

Ives, K. J., and C. S. B. Fitzpatrick (1989), Detachment of deposits from sand grains, *Colloids Surf.*, *39*, 239–253, doi:10.1016/0166-6622(89)80190-8.

Ives, K. J., and V. Pienvichitr (1965), Kinetics of the filtration of dilute suspensions, *Chem. Eng. Sci.*, *20*, 965–973, doi:10.1016/0009-2509(65)80094-X.

Johnson, H. P., M. Hutnak, R. P. Dziak, C. G. Fox, I. Urcuyo, J. P. Cowen, J. Nabelekk, and C. Fisher (2000), Earthquake-induced

changes in a hydrothermal system on the Juan de Fuca mid-ocean ridge, *Nature*, *407*, 174–177, doi:10.1038/35025040.

Jónsson, S., P. Segall, R. Pedersen, and G. Bjornsson (2003), Post-earthquake ground movements correlated to pore-pressure transients, *Nature*, *424*, 179–183, doi:10.1038/nature01776.

Kessler, J. H. (1993), Transport and channeling effects in a fracture partially clogged with colloidal material, Ph.D. thesis, Univ. of Calif., Berkeley.

Kim, J., and J. E. Tobiason (2004), Particles in filter effluent: The roles of deposition and detachment, *Environ. Sci. Technol.*, *38*, 6132–6138, doi:10.1021/es0352698.

King, C.-Y., D. Basler, T. S. Presser, W. C. Evans, and L. D. White (1994), In search of earthquake-related hydrologic and chemical changes along Hayward Fault, *Appl. Geochem.*, *9*, 83–91, doi:10.1016/0883-2927(94)90055-8.

Kitagawa, Y., K. Fujimori, and N. Koizumi (2007), Temporal change in permeability of the Nojima Fault zone by repeated water injection experiments, *Tectonophysics*, *443*, 183–192, doi:10.1016/j.tecto.2007.01.012.

Koizumi, N., W.-C. Lai, Y. Kitagawa, and Y. Matsumoto (2004), Comment on "Coseismic hydrological changes associated with dislocation of the September 21, 1999 Chichi earthquake, Taiwan" by Min Lee et al., *Geophys. Res. Lett.*, *31*, L13603, doi:10.1029/2004GL019897.

Kokusho, T. (2007), Liquefaction strengths of poorly graded and well-graded granular soils investigated by lab tests, in *Earthquake Geotechnical Engineering*, edited by K. D. Pililakis, pp. 159–184, Springer, New York, doi:10.1007/978-1-4020-5893-6_8.

Kouznetsov, O. L., E. M. Simkin, and G. V. Chilingar (1998), Improved oil recovery by application of vibro-energy to water-flooded sandstone, *J. Petrol. Sci. Eng.*, *19*, 191–200, doi:10.1016/S0920-4105(97)00022-3.

Kuribayashi, E., and F. Tatsuoka (1975), Brief review of liquefactions during earthquakes in Japan, *Soil Found.*, *15*, 81–92, doi:10.3208/sandf1972.15.4_81.

Lee, J.-C., H.-T. Chu, J. Angelier, Y.-C. Chan, J.-C. Hu, C.-Y. Lu, and R.-J. Rau (2002), Geometry and structure of northern rupture surface ruptures of the 1999 M_w = 7.6 Chi-Chi Taiwan earthquake: Influence from inherited fold belt structures, *J. Struct. Geol.*, *24*, 173–192, doi:10.1016/S0191-8141(01)00056-6.

Li, W., R. D. Vigil, I. A. Beresnev, P. Iassonov, and R. Ewing (2005), Vibration-induced mobilization of trapped oil ganglia in porous media: Experimental validation of a capillary-physics mechanism, *J. Colloid Interface Sci.*, *289*, 193–199, doi:10.1016/j.jcis.2005.03.067.

Liu, L. B., E. Roeloffs, and X. Y. Zheng (1989), Seismically induced water level oscillations in the Wali Well, Beijing, China, *J. Geophys. Res.*, *94*, 9453–9462, doi:10.1029/JB094iB07p09453.

Liu, W., and M. Manga (2009), Changes in permeability caused by dynamic stresses in fractured sandstone, *Geophys. Res. Lett.*, *36*, L20307, doi:10.1029/2009GL039852.

Logsdon, G. S., J. M. Symons, R. L. Hoye Jr., and M. M. Arozarena (1981), Alternative filtration methods for removal of Giardia cysts and cysts models, *J. Am. Water Works Assoc.*, *72*, 111–118.

Logsdon, G. S., L. Mason, and J. B. Stanley Jr. (1990), Trouble-shooting an existing treatment plant, *J. New Engl. Water Works Assoc.*, *104*(1), 43–56.

Majer, E., R. Baria, M. Stark, S. Oates, J. Bommer, B. Smith, and H. Asanuma (2007), Induced seismicity associated with enhanced geothermal systems, *Geothermics*, *36*, 185–222, doi:10.1016/j.geothermics.2007.03.003.

Manga, M. (2001), Origin of postseismic streamflow changes inferred from baseflow recession and magnitude-distance relation, *Geophys. Res. Lett.*, *28*, 2133–2136, doi:10.1029/2000GL012481.

Manga, M., and J. C. Rowland (2009), Response of Alum Rock springs to the October 30, 2007 Alum Rock earthquake and implications for the origin of increased discharge after

earthquakes, *Geofluids*, *9*, 237–250, doi:10.1111/j.1468-8123.2009.00250.x.

Manga, M., E. E. Brodsky, and M. Boone (2003), Response of stream flow to multiple earthquakes, *Geophys. Res. Lett.*, *30*(5), 1214, doi:10.1029/2002GL016618.

Manga, M., M. Brumm, and M. L. Rudolph (2009), Earthquake triggering of mud volcanoes, *J. Mar. Petrol. Geol.*, *26*, 1785–1798, doi:10.1016/j.marpetgeo.2009.01.019.

Manning, C. E., and S. E. Ingebritsen (1999), Permeability of the continental crust: The implications of geothermal data and metamorphic system, *Rev. Geophys.*, *37*, 127–150, doi:10.1029/1998RG900002.

Mays, D. C. (2007), Using the Quirk-Schofield diagram to explain environmental colloid dispersion phenomena, *J. Nat. Resour. Life Sci. Educ.*, *36*, 45–52.

Mays, D. C. (2010), Contrasting clogging in granular media filters, soils, and dead-end membranes, *J. Environ. Eng.*, *136*, 475–480, doi:10.1061/(ASCE)EE.1943-7870.0000173.

Mays, D. C., and J. R. Hunt (2007), Hydrodynamic and chemical factors in clogging by montmorillonite in porous media, *Environ. Sci. Technol.*, *41*, 5666–5671, doi:10.1021/es062009s.

McGarr, A., D. Simpson, and L. Seeber (2002), Case histories of induced and triggered seismicity, in *International Handbook of Earthquake and Engineering Seismology*, edited by W. H. K. Lee et al., pp. 647–661, Academic, Amsterdam, doi:10.1016/S0074-6142(02)80243-1.

Mellors, R., D. Kilb, A. Aliyev, A. Gasanov, and G. Yetirmishli (2007), Correlations between earthquakes and large mud volcano eruptions, *J. Geophys. Res.*, *112*, B04304, doi:10.1029/2006JB004489.

Melrose, J. C., and C. F. Brandner (1974), Role of capillary forces in determining microscopic displacement efficiency for oil recovery by waterflooding, *J. Can. Pet. Tech.*, *13*, 54–62.

Miller, S. A., C. Collettini, L. Chiaraluce, M. Cocco, M. Barchi, and B. J. P. Kaus (2004), Aftershocks driven by a high-pressure CO_2 source at depth, *Nature*, *427*, 724–727, doi:10.1038/nature02251.

Mogi, K., H. Mochizuki, and Y. Kurokawa (1989), Temperature changes in an artesian spring at Usami in the Izu Peninsula (Japan) and their relation to earthquakes, *Tectonophysics*, *159*, 95–108, doi:10.1016/0040-1951(89)90172-8.

Montgomery, D. R., H. M. Greenberg, and D. T. Smith (2003), Streamflow response to the Nisqually earthquake, *Earth Planet. Sci. Lett.*, *209*, 19–28, doi:10.1016/S0012-821X(03)00074-8.

Moore, D. E., D. A. Lockner, and J. A. Byerlee (1994), Reduction of permeability in granite at elevated temperatures, *Science*, *265*, 1558–1561, doi:10.1126/science.265.5178.1558.

Muir-Wood, R., and G. C. P. King (1993), Hydrological signatures of earthquake strain, *J. Geophys. Res.*, *98*, 22,035–22,068, doi:10.1029/93JB02219.

National Research Council (1985), *Liquefaction of Soils During Earthquakes*, 240 pp., Natl. Acad., Washington, D. C.

Neuzil, C. E. (1995), Abnormal pressures as hydrodynamic phenomena, *Am. J. Sci.*, *295*, 742–786, doi:10.2475/ajs.295.6.742.

Nikolaevskiy, V. N., G. P. Lopukhov, Y. Liao, and M. J. Economides (1996), Residual oil reservoir recovery with seismic vibrations, *SPE Prod. Facil.*, *11*, 89–94, doi:10.2118/29155-PA.

Ohtake, M. (1974), Seismic activity induced by water injection at Matsuhiro, Japan, *J. Phys. Earth*, *22*, 163–176, doi:10.4294/jpe1952.22.163.

Papadopoulos, G. A., and G. Lefkopoulos (1993), Magnitude-distance relations for liquefaction in soil from earthquakes, *Bull. Seismol. Soc. Am.*, *83*, 925–938.

Poesio, P., G. Ooms, M. E. H. van Dongen, and D. M. J. Smeulders (2004), Removal of small particles from a porous material by ultrasonic irradiation, *Transp. Porous Media*, *54*, 239–364, doi:10.1023/B:TIPM.0000003677.35458.63.

Polak, A., D. Elsworth, H. Yasuhara, A. S. Grader, and P. M. Halleck (2003), Permeability reduction of a natural fracture under

net dissolution by hydrothermal fluids, *Geophys. Res. Lett.*, *30*(20), 2020, doi:10.1029/2003GL017575.

Polak, A., D. Elsworth, J. Liu, and A. Grader (2004), Spontaneous switching of permeability changes in a limestone fracture under net dissolution, *Water Resour. Res.*, *40*, W03502, doi:10.1029/2003WR002717.

Quirk, J. P., and R. K. Schofield (1955), The effect of electrolyte concentration on soil permeability, *J. Soil Sci.*, *6*, 163–178, doi:10.1111/j.1365-2389.1955.tb00841.x.

Raleigh, C. B., J. H. Healy, and J. D. Bredehoeft (1976), An experiment in earthquake control at Rangely, Colorado, *Science*, *191*, 1230–1237.

Roberts, P. M. (2005), Laboratory observations of altered porous fluid flow behavior in Berea sandstone induced by low-frequency dynamic stress stimulation, *Acoust. Phys.*, *51*, 140–148, doi:10.1134/1.2133962.

Roberts, P. M., and A. I. Abdel-Fattah (2009), Seismic stress stimulation mobilizes colloids trapped in a porous rock, *Earth Planet. Sci. Lett.*, *284*, 538–543, doi:10.1016/j.epsl.2009.05.017.

Roberts, P. M., I. B. Esipov, and E. L. Majer (2003), Elastic wave stimulation of oil reservoirs: Promising EOR technology?, *Leading Edge*, *22*, 448–453, doi:10.1190/1.1579578.

Roeloffs, E. A. (1998), Persistent water level changes in a well near Parkfield, California, due to local and distant earthquakes, *J. Geophys. Res.*, *103*, 869–889, doi:10.1029/97JB02335.

Rojstaczer, S., and S. Wolf (1992), Permeability changes associated with large earthquakes: An example from Loma Prieta, California, 10/17/89 earthquake, *Geology*, *20*, 211–214, doi:10.1130/0091-7613(1992)020<0211:PCAWLE>2.3.CO;2.

Rudolph, M. L., and M. Manga (2010), Mud volcano response to the 4 April 2010 El Mayor-Cucapah earthquake, *J. Geophys. Res.*, *115*, B12211, doi:10.1029/2010JB007737.

Saar, M. O., and M. Manga (2004), Depth dependence of permeability in the Oregon Cascades inferred from hydrogeologic, thermal, seismic, and magmatic modeling constraints, *J. Geophys. Res.*, *109*, B04204, doi:10.1029/2003JB002855.

Sato, T., R. Sakai, K. Furuya, and T. Kodama (2000), Coseismic spring flow changes associated with the 1995 Kobe earthquake, *Geophys. Res. Lett.*, *27*, 1219–1222, doi:10.1029/1999GL011187.

Seed, H. B. (1968), Landslides during earthquakes due to soil liquefaction, *J. Soil Mech. Found. Div. Am. Soc. Civ. Eng.*, *94*, 1055–1122.

Shapiro, S. A., and C. Dinske (2009), Fluid-induced seismicity: Pressure diffusion and hydraulic fracturing, *Geophys. Prospect.*, *57*, 301–310, doi:10.1111/j.1365-2478.2008.00770.x.

Shapiro, S. A., C. Dinske, C. Langenbruch, and F. Wenzel (2010), Seismogenic index and magnitude probability of earthquakes induced during reservoir fluid stimulations, *Leading Edge*, *29*, 304–309, doi:10.1190/1.3353727.

Shi, Y.-L., J. L. Cao, L. Ma, and B. J. Yin (2007), Tele-seismic coseismic well temperature changes and their interpretation, *Acta Seismol. Sinica*, *20*, 280–289.

Shmonov, V. M., V. M. Vitovtova, and A. V. Zharikov (1999), Experimental study of seismic oscillation effect on rock permeability under high temperature and pressure, *Int. J. Rock Mech. Min. Sci.*, *36*, 405–412, doi:10.1016/S0148-9062(99)00020-0.

Shmonov, V. M., V. M. Vitiovtova, A. V. Zharikov, and A. A. Grafchikov (2002), Fluid permeability of the continental crust: Estimation from experimental data, *Geochem. Int.*, *40*(1), 3–13.

Shmonov, V. M., V. M. Vitiovtova, A. V. Zharikov, and A. A. Grafchikov (2003), Permeability of the continental crust: Implications of experimental data, *J. Geochem. Explor.*, *78–79*, 697–699, doi:10.1016/S0375-6742(03)00129-8.

Sibson, R. (1990), Rupture nucleation on unfavorably oriented faults, *Bull. Seismol. Soc. Am.*, *80*, 1580–1604.

Stober, I., and K. Bucher (2007), Hydraulic properties of the crystalline basement, *Hydrogeol. J.*, *15*, 213–224, doi:10.1007/s10040-006-0094-4.

Sumita, I., and M. Manga (2008), Suspension rheology under oscillatory shear and its geophysical implications, *Earth Planet. Sci. Lett.*, *269*, 468–477, doi:10.1016/j.epsl.2008.02.043.

Taber, J. J. (1969), Dynamic and static forces required to remove a discontinuous oil phase from porous media containing both oil and water, *Soc. Pet. Eng. J.*, *9*, 3–12, doi:10.2118/2098-PA.

Talwani, P., and S. Acree (1985), Pore pressure diffusion and the mechanism of reservoir-induced seismicity, *Pure Appl. Geophys.*, *122*, 947–965, doi:10.1007/BF00876395.

Talwani, P., L. Chen, and K. Gahalaut (2007), Seismogenic permeability, k_s, *J. Geophys. Res.*, *112*, B07309, doi:10.1029/2006JB004665.

Taron, J., and D. Elsworth (2010), Constraints on compaction rate and equilibrium in the pressure solution creep of quartz aggregates and fractures: Controls of aqueous concentration, *J. Geophys. Res.*, *115*, B07211, doi:10.1029/2009JB007118.

Tchobanoglous, G., and F. L. Burton (1991), *Wastewater Engineering: Treatment, Disposal, and Reuse*, 1334 pp., McGraw-Hill, New York.

Thomas, J. M., and C. V. Chrysikopoulos (2007), Experimental investigation of acoustically enhanced colloid transport in water-saturated packed columns, *J. Colloid Interface Sci.*, *308*, 200–207, doi:10.1016/j.jcis.2006.12.062.

Tokunaga, T. (1999), Modeling of earthquake induced hydrological changes and possible permeability enhancement due to the 17 January 1995 Kobe earthquake, Japan, *J. Hydrol.*, *223*, 221–229, doi:10.1016/S0022-1694(99)00124-9.

Townend, J., and M. D. Zoback (2000), How faulting keeps the crust strong, *Geology*, *28*, 399–402, doi:10.1130/0091-7613(2000)28<399:HFKTCS>2.0.CO;2.

Tsunogai, U., and H. Wakita (1995), Precursory chemical changes in groundwater: Kobe earthquake, Japan, *Science*, *269*, 61–63, doi:10.1126/science.269.5220.61.

van der Elst, N. J., and E. E. Brodsky (2010), Connecting near-field and far-field earthquake triggering to dynamic strain, *J. Geophys. Res.*, *115*, B07311, doi:10.1029/2009JB006681.

Veerapaneni, S., and M. R. Wiesner (1997), Deposit morphology and head loss development in porous media, *Environ. Sci. Technol.*, *31*, 2738–2744, doi:10.1021/es960979h.

Wakita, H., G. Igarashi, Y. Nakamura, Y. Sano, and K. Notsu (1989), Coseismic radon changes in groundwater, *Geophys. Res. Lett.*, *16*, 417–420, doi:10.1029/GL016i005p00417.

Waller, R. M., H. E. Thomas, and R. C. Vorhis (1965), Effects of the Good Friday earthquake on water supplies, *J. Am. Water Works Assoc.*, *57*, 123–131.

Wan, J., and J. L. Wilson (1994), Visualization of the role of the gas-water interface on the fate and transport of colloids in porous media, *Water Resour. Res.*, *30*, 11–23, doi:10.1029/93WR02403.

Wang, C.-Y. (2007), Liquefaction beyond the near field, *Seismol. Res. Lett.*, *78*, 512–517, doi:10.1785/gssrl.78.5.512.

Wang, C.-Y., and Y. Chia (2008), Mechanisms of water level changes during earthquakes: Near field versus intermediate field, *Geophys. Res. Lett.*, *35*, L12402, doi:10.1029/2008GL034227.

Wang, C.-Y., and M. Manga (2010a), Hydrologic responses to earthquakes–A general metric, *Geofluids*, *10*, 206–216.

Wang, C.-Y., and M. Manga (2010b) *Earthquakes and Water*, Lecture Notes Earth Sci. Ser., vol. 114, 249 pp., Springer, Berlin.

Wang, C.-Y., L. H. Cheng, C. V. Chin, and S. B. Yu (2001), Coseismic hydrologic response of an alluvial fan to the 1999 Chi-Chi earthquake, Taiwan, *Geology*, *29*, 831–834, doi:10.1130/0091-7613(2001)029<0831:CHROAA>2.0.CO;2.

Wang, C.-Y., D. S. Dreger, C.-H. Wang, D. Mayeri, and J. G. Berryman (2003), Field relations among coseismic ground motion, water level change, and liquefaction for the 1999 Chi-Chi (M_w = 7.5) earthquake, Taiwan, *Geophys. Res. Lett.*, *30*(17), 1890, doi:10.1029/2003GL017601.

Wang, C.-Y., C. H. Wang, and M. Manga (2004), Coseismic release of water from mountains: Evidence from the 1999(M_w =

7.5) Chi-Chi, Taiwan, earthquake, *Geology*, *32*, 769–772, doi:10.1130/G20753.1.

Wang, C.-Y., Y. Chia, O.-L. Wang, and D. Dreger (2009), Role of S waves and Love waves in coseismic permeability enhancement, *Geophys. Res. Lett.*, *36*, L09404, doi:10.1029/2009GL037330.

Wang, C.-Y., M. Manga, C.-H. Wang, and C.-H. Chin (2012), Earthquakes and subsurface temperature changes near an active mountain front, *Geology*, *40*, 119–122, doi:10.1130/G32565.1.

West, M., J. J. Sanchez, and S. McNutt (2005), Periodically triggered seismicity at Mount Wrangell, Alaska, after the Sumatra earthquake, *Science*, *308*, 1144–1146, doi:10.1126/science.1112462.

Whitehead, R. L., R. W. Harper, and H. G. Sisco (1984), Hydrologic changes associated with the October 28, 1983 Idaho earthquake, *Pure Appl. Geophys.*, *122*, 280–293, doi:10.1007/BF00874599.

Wong, A., and C.-Y. Wang (2007), Field relations between the spectral composition of ground motion and hydrological effects during the 1999 Chi-Chi (Taiwan) earthquake, *J. Geophys. Res.*, *112*, B10305, doi:10.1029/2006JB004516.

Yardley, B. W. D., and L. P. Baumgartner (2007), Fluid processes in deep crustal fault zones, in *Tectonic Faults–Agents of Change on a Dynamic Earth*, edited by M. R. Handy, G. Hirth, and N. Hovius, pp. 295–318, MIT Press, Cambridge, U. K.

Yasuhara, H., and D. Elsworth (2008), Compaction of a fracture moderated by competing roles of stress corrosion and pressure solution, *Pure Appl. Geophys.*, *165*, 1289–1306, doi:10.1007/s00024-008-0356-2.

Yasuhara, H., D. Elsworth, and A. Polak (2003), A mechanistic model for compaction of granular aggregates moderated by pressure solution, *J. Geophys. Res.*, *108*(B11), 2530, doi:10.1029/2003JB002536.

Yasuhara, H., D. Elsworth, and A. Polak (2004), The evolution of permeability in a natural fracture: Significant role of pressure solution, *J. Geophys. Res.*, *109*, B03204, doi:10.1029/2003JB002663.

Yasuhara, H., A. Polak, Y. Mitani, A. Grader, P. Halleck, and D. Elsworth (2006), Evolution of fracture permeability through fluid-rock reaction under hydrothermal conditions, *Earth Planet. Sci. Lett.*, *244*, 186–200, doi:10.1016/j.epsl.2006.01.046.

Yoshimi, Y., and H. Oh-Oka (1975), Influence of degree of shear stress reversal on the liquefaction potential of saturated sand, *Soil Found.*, *15*, 27–40, doi:10.3208/sandf1972.15.3_27.

Youd, T. L., and B. L. Carter (2005), Influence of soil softening and liquefaction on spectral acceleration, *J. Geotech. Geoenviron. Eng.*, *131*, 811–825, doi:10.1061/(ASCE)1090-0241(2005)131:7(811).

Youd, T. L., E. L. Harp, D. K. Keefer, and R. C. Wilson (1985), The Borah Peak, Idaho, earthquake of October 28, 1983–Liquefaction, *Earthquake Spectra*, *2*, 71–89, doi:10.1193/1.1585303.

Zhang, S., S. Cox, and M. Paterson (1994), The influence of room temperature deformation on porosity and permeability in calcite aggregates, *J. Geophys. Res.*, *99*, 15,761–15,775, doi:10.1029/94JB00647.

Zoback, M. D. (2007), *Reservoir Geomechanics*, Cambridge Univ. Press, Cambridge, U. K., doi:10.1017/CBO9780511586477.